Cellular/Molecular

Lewis^x and α2,3-Sialyl Glycans and Their Receptors TAG-1, Contactin, and L1 Mediate CD24-Dependent Neurite Outgrowth

Annika Lieberoth,[1]* Frauke Splittstoesser,[1]* Nainesh Katagihallimath,[1] Igor Jakovcevski,[1] Gabriele Loers,[1] Barbara Ranscht,[2] Domna Karagogeos,[3] Melitta Schachner,[1,4,5] and Ralf Kleene[1]

[1]Zentrum für Molekulare Neurobiologie, Universitätsklinikum Hamburg-Eppendorf, 20246 Hamburg, Germany, [2]Burnham Institute for Medical Research, La Jolla, California 92037, [3]Department of Basic Science, Medical School and Institute of Molecular Biology and Biotechnology, University of Crete, 71110 Heraklion, Greece, [4]Keck Center for Collaborative Neuroscience, Rutgers University, Piscataway, New Jersey 08854, and [5]Center for Neuroscience, Shantou University Medical College, Shantou 515041, China

Although carbohydrates have been implicated in cell interactions in the nervous system, the molecular bases of their functions have remained largely obscure. Here, we show that promotion or inhibition of neurite outgrowth of cerebellar or dorsal root ganglion neurons, respectively, induced by the mucin-type adhesion molecule CD24 depends on α2,3-linked sialic acid and Lewis^x present on glia-specific CD24 glycoforms. α2,3-Sialyl residues of CD24 bind to a structural motif in the first fibronectin type III domain of the adhesion molecule L1. Following the observation that the adhesion molecules TAG-1 and Contactin show sequence homologies with fucose-specific lectins, we obtained evidence that TAG-1 and Contactin mediate Lewis^x-dependent CD24-induced effects on neurite outgrowth. Thus, L1, TAG-1, and Contactin function as lectin-like neuronal receptors. Their *cis* interactions with neighboring adhesion molecules, e.g., Caspr1 and Caspr2, and with their triggered signal transduction pathways elicit cell type-specific promotion or inhibition of neurite outgrowth induced by glial CD24 in a glycan-dependent *trans* interaction.

Introduction

Glycans have increasingly been recognized as important players in cell–cell interactions. In the nervous system, diverse functions depending on cell recognition, such as cell migration, neurite outgrowth and fasciculation, synapse formation and stabilization, and modulation of synaptic efficacy are mediated by distinct carbohydrate structures (for review, see Kleene and Schachner, 2004). Glycoproteins, proteoglycans and highly *O*-glycosylated mucins as well as glycolipids have all been identified to carry functionally important glycan structures (for reviews, see Haltiwanger and Lowe, 2004; Kleene and Schachner, 2004).

The Lewis^x epitope (CD15) and α2,3-sialyl glycans have only been studied sparsely in the nervous system. Lewis^x is present on *O*- and *N*-linked glycans in the nervous system (Chen et al., 1998; Chai et al., 1999), where its expression is temporally and spatially regulated during development (Gocht et al., 1996; Mai et al., 1999) and where it is implicated in cell adhesion, migration and neurite outgrowth (Sajdel-Sulkowska, 1998; Brito et al., 2007).

α2,3-Linked sialic acid binds to the myelin associated glycoprotein MAG, which belongs to the sialic acid binding Ig-like lectin family (siglec) (Crocker et al., 1998). Removal of sialic acid residues from nerve cells or mutation of the sialic acid binding site in MAG reverses the MAG-mediated inhibition of neurite outgrowth (Vinson et al., 1996, 2001). A putative binding domain for α2,3-linked sialic acid was also identified in the cell adhesion molecule L1 (Kleene et al., 2001).

The cell adhesion molecule CD24 is a highly glycosylated mucin with a peptide core of only 27 aa whose functions are mainly if not exclusively mediated by its carbohydrates. Its expression is tightly regulated during nervous system development (Kleene et al., 2001; and references therein). CD24 is known to mediate cell adhesion (Kadmon et al., 1992; Nielsen et al., 1997) and neurite outgrowth (Shewan et al., 1996; Kleene et al., 2001).

L1 is a glycan-binding and -carrying adhesion molecule that is important for neuronal migration, neurite outgrowth, axon guidance and fasciculation, neuronal survival, synaptic plasticity, myelination, and remyelination after injury (for review, see Maness and Schachner, 2007). L1 interacts homophilically and heterophilically with other cell adhesion proteins of the Ig-superfamily, e.g., TAG-1/axonin-1 and F3/Contactin (hereafter called TAG-1 and Contactin) (for review, see Karagogeos, 2003; Haspel and Grumet, 2003; Sonderegger, 1997; Falk et al., 2002). In light of the complex modes of interactions between these adhesion molecules, it appears timely to further characterize the

Received Sept. 12, 2008; revised Feb. 24, 2009; accepted March 3, 2009.

This work was supported by the Deutsche Forschungsgemeinschaft (Grants KL-1378/1-1, 1-2, 2-1, and 2-2). We are grateful to Genevieve Rougon for Contactin-expressing cells and plasmids, Zhi-Cheng Xiao for Fc-proteins, Elior Peles for Caspr-deficient mice, Peter Altevogt for CD24 antibody-producing hybridoma cells, Emanuela Szpotowicz and Laura Hoelters for technical assistance, and Ulrike Wolters, Tanja Stößner, Ali Derin, and Eva Kronberg for breeding and maintenance of mice.

*A.L. and F.S. contributed equally to this work.

Correspondence should be addressed to Melitta Schachner, Zentrum für Molekulare Neurobiologie, Universitätsklinikum Hamburg-Eppendorf, Martinistrasse 52, D-20246 Hamburg, Germany. E-mail: melitta.schachner@zmnh.uni-hamburg.de.

DOI:10.1523/JNEUROSCI.4361-08.2009

 0270-6474/09/296677-14$15.00/0

molecular bases and functional consequences of such interactions from the point of view that these molecules may be both donors and acceptors of functionally decisive glycan structures.

In the current study, we show that CD24 affects neurite outgrowth via its α2,3-sialyl and Lewis^x glycans. We identified the binding motif for α2,3-sialyl residues in a siglec homologous sequence in L1 and obtained indications for Lewis^x-mediated interactions of CD24 with TAG-1 and Contactin. Since the functions of CD24 are conferred most likely by its glycans, the present findings exemplify that carbohydrates play important roles in modulating developmentally important processes depending on cell adhesion, such as neurite outgrowth.

Materials and Methods

Animals. C57BL/6J mice were used as wild-type mice. TAG-1-deficient mice (Fukamauchi et al., 2001) were kept as homozygous breeding pairs. Wild-type littermates were used as controls. Caspr1-deficient mice (Bhat et al., 2001), which were generously provided by Elior Peles (Weizmann Institute of Science, Rehovot, Israel), Contactin-deficient mice (Berglund et al., 1999), and CD24-deficient mice (Wenger et al., 1995) were maintained as heterozygous breeding pairs. Contactin-deficient mice were maintained on a mixed genetic background (129SVJ × C57BL/6 × Black Swiss), and TAG-1- and Caspr1-deficient mice on an inbred C57BL/6J background. CD24-deficient mice were on a CD1 background. All experiments were conducted in accordance with the German and European Community laws on protection of experimental animals, and all procedures used were approved by the responsible committee of The State of Hamburg.

Antibodies and reagents. Polyclonal antibodies to mouse L1 (Chen et al., 1999), NCAM (Kadmon et al., 1992), Contactin (R&D Systems), TAG-1 [TG3, Traka et al., (2003) and from R&D Systems], Caspr1 (Santa Cruz Biotechnology), and Caspr2 (Santa Cruz Biotechnology) and monoclonal antibodies to mouse CD24 [79; Kadmon et al. (1992)], oligomannosides, HNK-1 (for reference, see Heller et al., 2003), and Lewis^x (Streit et al., 1996) were used. Carbohydrates and glycoconjugates were purchased from Dextra Laboratories, peptide *N*-glycosidase F (PNGase F) from Roche Molecular Biochemicals, and *O*-sialoglycoprotein endopeptidase (OSGE) of *Mannheimia hemolytica* from Cedarline. Recombinant L1 protein fragments (Ig I-VI, FN 1-5, FN 1-2, and FN 3-5) were produced in *Escherichia coli* as described previously (Appel et al., 1993) and purified by using the Whole Gel Eluter from Bio-Rad. Biotinylated L1 peptide and its scrambled peptide were from Schafer-N. CD24 was purified from early postnatal mouse brain as described previously (Kleene et al., 2001).

Binding assays. ELISA based binding tests were performed as described (Kleene et al., 2001). For substrate-coating, 5 μg/ml CD24 were used. L1 protein fragments or biotinylated L1 peptides were diluted in buffer A (TBS, 1% BSA, 1 mM $CaCl_2$, 1 mM $MgCl_2$, 1 mM $MnCl_2$) containing 0.05% Tween 20. In competition assays, the recombinant L1 fragment was preincubated for 2 h with the carbohydrates. Polyclonal L1 and HRP-coupled secondary antibodies (Dianova) or HRP-coupled streptavidin (Sigma) in buffer A with 0.05% Tween 20 were used for detection.

Enzymatic digestion of CD24. Purified CD24 was incubated overnight with 2 U PNGase F at 37°C in 20 mM sodium phosphate, pH 7.2, containing 0.5% CHAPS or with OSGE in 50 mM HEPES, pH 7.4, for 4 h at 37°C. The digested protein was further analyzed by Western blotting.

Chinese hamster ovary cell culture and transfection. Chinese hamster ovary (CHO) cells stably transfected with TAX-1, the human homolog of TAG-1 (Pavlou et al., 2002), were grown in Glasgow's Minimal Essential Medium with supplements [10% FCS, 2 mM L-glutamine, nonessential amino acids, 0.1 mg/ml streptomycin, 10 U/ml penicillin, 1× glutamate/aspartate (Sigma)]. CHO cells were transfected with pCDNA3 vectors coding for mouse Contactin (Buttiglione et al., 1996) or rat NCAM120 (Niethammer et al., 2002) using Lipofectamine (Invitrogen). Stably transfected cells were selected by adding 0.3–0.4 mg/ml G418 (PAA Laboratories).

Primary cell culture. Cerebellar and DRG neurons were prepared from 5- to 7-d-old wild-type, TAG-1-, Contactin-, or Caspr-deficient mice as described previously (Chen et al., 1999; Kleene et al., 2001). Hippocampal neurons were prepared from 1- to 2-d-old wild-type mice (Dityatev et al., 2007) and neurons from spinal cord were prepared from 14-d-old wild-type embryos (Simova et al., 2006). Cortical neurons were prepared from 17-d-old wild-type embryos. Briefly, the cerebral cortex was isolated, cleaned from meninges and digested for 30 min at 37°C using 0.05% trypsin in HBSS. Cortices were washed with HBSS containing 10% BSA and 1% trypsin inhibitor and dissociated using fire polished Pasteur pipettes. Dissociated cells were grown in glutamine containing Neurobasal medium (Invitrogen) with B27 supplement and 0.5% penicillin/streptomycin. For neurite outgrowth assays, dissociated cerebellar neurons ($1–2 \times 10^5$ cells/ml), DRG neurons (1×10^4 cells/ml), hippocampal neurons (1×10^5 cells/ml) or cortical neurons (2×10^5 cells/ml) were seeded onto glass coverslips precoated with 0.1 mg/ml poly-L-lysine (PLL) or with PLL and 5 μg/ml CD24 or 10 μg/ml laminin (Santa Cruz Biotechnology). Spinal cord neurons (1×10^5 cells/ml) were seeded onto glass coverslips precoated with 0.015 mg/ml poly-L-ornithine (PLO) or with PLO and 5 μg/ml CD24. A 100 μM concentration of 3′-sialyl-*N*-acetyllactosamine or 6′-sialyl-*N*-acetyllactosamine, 10 μM Lewis^x or Lewis^a or antibodies L5 (1:100), 412 (1 μg/ml), or against NCAM (5 μg/ml), Contactin (1:1000), TAG-1 (1:1000), Caspr1 (1:1000), or Caspr2 (1:1000) were added 1 h after seeding the cells. After 20–24 h, cells were fixed by adding 2.5% glutaraldehyde and stained with 1% toluidine blue, 1% methylene blue in 1% borax. Neurite outgrowth was quantified by measuring total neurite length of 100 cerebellar neurons, hippocampal neurons, spinal cord and cortical non-motoneurons and spinal cord motoneurons, or of 50–100 DRG neurons or cortical motoneurons using an AxioVision system 4.6 (Carl Zeiss). Spinal and cortical neurons showing a large triangular cell body with an edge length of 15–20 μm were taken as motoneurons, while round spinal and cortical neurons with a diameter of ~10 μm were taken as non-motoneurons. Data from at least three independent experiments were analyzed applying Student's *t* test.

Primary cell culture of astrocytes was performed as described by Kleene et al. (2007). For Western blot analysis, cerebellar neurons or astrocytes cultured for 20–24 h were washed in PBS and treated with lysis buffer (50 mM Tris/HCl, pH 7.4, 150 mM NaCl, 1 mM EDTA, 1% NP-40). After centrifugation ($1000 \times g$, 10 min, 4°C) SDS sample buffer was added.

Coupling of CD24 to Fluospheres and binding to cells. Purified CD24 was coupled to carboxylate-modified fluorescent microspheres (Fluospheres Crimson, Invitrogen) by activation via EDAC. For control, Fluospheres were activated and quenched by glycine only (unconjugated control beads). Before being added to the cells, Fluospheres were sonicated and diluted in Ham's F12 to prevent aggregation. Dissociated DRG neurons were seeded onto PLL coverslips. After 42–48 h, CD24 or unconjugated Fluospheres were added to the cells (5 μl/ml medium) and incubated for 1 h at 37°C. Unbound Fluospheres were removed by three washes with Ham's F12 and immunocytochemistry was performed.

Immunocytochemistry. Dissociated DRG neurons were seeded onto PLL coverslips. After 42–48 h, cells were fixed with 4% paraformaldehyde [20 min, room temperature (RT)]. After blocking with 3% BSA in PBS (1 h, RT) cells were incubated with polyclonal antibodies against L1 (1:500), TAG-1 (1:15), Contactin (1:10), Caspr (1:50), or Caspr2 (1:50) diluted in 3% BSA in PBS (overnight, 4°C) and with Cy2-conjugated donkey anti-rabbit and Cy3-conjugated donkey anti-goat antibodies (Dianova, each 1:200) for 2 h at RT. Coverslips were embedded in Aqua-Poly/Mount (Polysciences). Confocal microscope analysis was performed using a Leica Microscope (DM IRBE, Leica Microsystems). Images were acquired at RT using Leica Confocal Software V 2.61 and an oil HCX PL APO 40×/1.25 objective (Leica). Contrast and brightness were further adjusted in Adobe Photoshop CS (Adobe Systems).

Pull-down assay and immunoprecipitation. For pull-down assays, 80 μg of Lewis^x–BSA, *N*-acetyllactosamine–BSA, or BSA (Sigma) was coated onto Dynabeads M-270 Epoxy (Dynal) by overnight incubation at 4°C. Transfected CHO cells were homogenized in buffer A (50 mM Tris/HCl, pH 7.5, 1 mM $CaCl_2$, 1 mM $MgCl_2$) and centrifuged at $1000 \times g$ for 10 min. Supernatants were applied to beads and incubated overnight at 4°C. Purified CD24 was coated onto Dynabeads M-270 Epoxy by incubation

at 37°C for 24 h. Purified TAX-1-Fc, Contactin-Fc (generously provided by Zhi-Cheng Xiao, Institute of Molecular and Cell Biology, Singapore), CHL1-Fc (Chen et al., 1999), or Fc (Athens Research & Technology) were incubated with the CD24 beads. Beads were washed three times each with buffer A containing 0.1% Triton X-100 and buffer A and boiled in SDS sample buffer.

For immunoprecipitation, brains or cerebellar tissue from 5- to 7-d-old C57BL/6J mice were homogenized in buffer A containing 0.32 M sucrose. After centrifugation at 1000 × *g* for 10 min and 17,000 × *g* for 20 min the resulting pellet was resuspended in buffer A containing 0.1% Triton X-100. After preclearing, samples were incubated overnight at 4°C with CD24 antibody (5 μg), TAG-1 antibody (0.5 μg), Contactin antibody (0.5 μg) or, as controls, with corresponding amounts of nonimmune control IgG (Jackson ImmunoResearch Laboratories) and with Protein G coupled magnetic beads (Perbio) for 7 h. Beads were washed three times each with buffer A containing 1% Triton X-100 and buffer A and boiled in SDS sample buffer.

Spinal cord injury. Mice were anesthetized by intraperitoneal injections of 100 mg of Ketanest (Parke-Davis/Pfizer) and 5 mg of Rompun (Bayer) per kilogram of body weight. Laminectomy was performed at the T7–T9 level with mouse laminectomy forceps (Fine Science Tools). A mouse spinal cord compression device was used for compression injury (Curtis et al., 1993). Compression force (degree of closure of the forceps) and duration were controlled by an electromagnetic device. The spinal cord was maximally compressed (100%, according to the operational definition of Curtis et al., 1993) for 1 s by a time-controlled current flow through the electromagnetic device. The skin was then surgically closed using 6–0 nylon stitches (Ethicon). After the surgery, mice were kept in a heated room (35°C) for several hours to prevent hypothermia and then singly housed in a temperature-controlled (22°C) room with water and standard food provided *ad libitum*. The bladders of the animals were manually voided twice daily. Animals were carefully observed for general health and well being No signs of pain were detectable throughout the duration of the experiments.

Analysis of motor function. The recovery of ground locomotion was evaluated using the Basso Mouse Scale (BMS) rating scale (Basso et al., 2006), and a novel single-frame motion analysis (Apostolova et al., 2006). This method includes evaluation of four parameters in three different tests: beam walking (foot-stepping angle and rump-height index), voluntary movements without body weight support (extension-flexion ratio), and inclined ladder climbing (number of correct steps). Assessment was performed before, and at 1, 3, and 6 weeks after the injury. Values for the left and right legs were averaged.

Histological analysis of the spinal cords. Mice were transcardially perfused with fixative consisting of 4% formaldehyde and 0.1% $CaCl_2$ in 0.1 M cacodylate buffer, pH 7.3, for 15 min at room temperature. After perfusion, the spinal cords were dissected out and postfixed overnight at 4°C in the same solution as used for perfusion, and then cryoprotected in 15% sucrose solution in 0.1 M cacodylate buffer, pH 7.3, for 2 d at 4°C. Pieces of spinal cords 1 cm in length centered at the lesion site were embedded in Tissue Tek (Sakura Finetek), and frozen by 2 min immersion into 2-methyl-butane (isopentane) precooled to −80°C. Serial longitudinal sections were cut in a cryostat (CM3050; Leica) and 25-μm-thick sections were collected on SuperFrost Plus glass slides (Roth). Immunofluorescence labeling of the spinal cord tissue with anti-neurofilament (NF; Millipore, 1:2000) and anti-tyrosine hydroxylase (TH; Millipore, 1:800) antibodies was performed as described (Jakovcevski et al., 2007). Number of axons was counted directly under the Axiophot (Zeiss) microscope using the Neurolucida software (MicroBrightField). Representative images were taken by Axiophot (Zeiss) microscope and processed in Photoshop C2 (Adobe Systems).

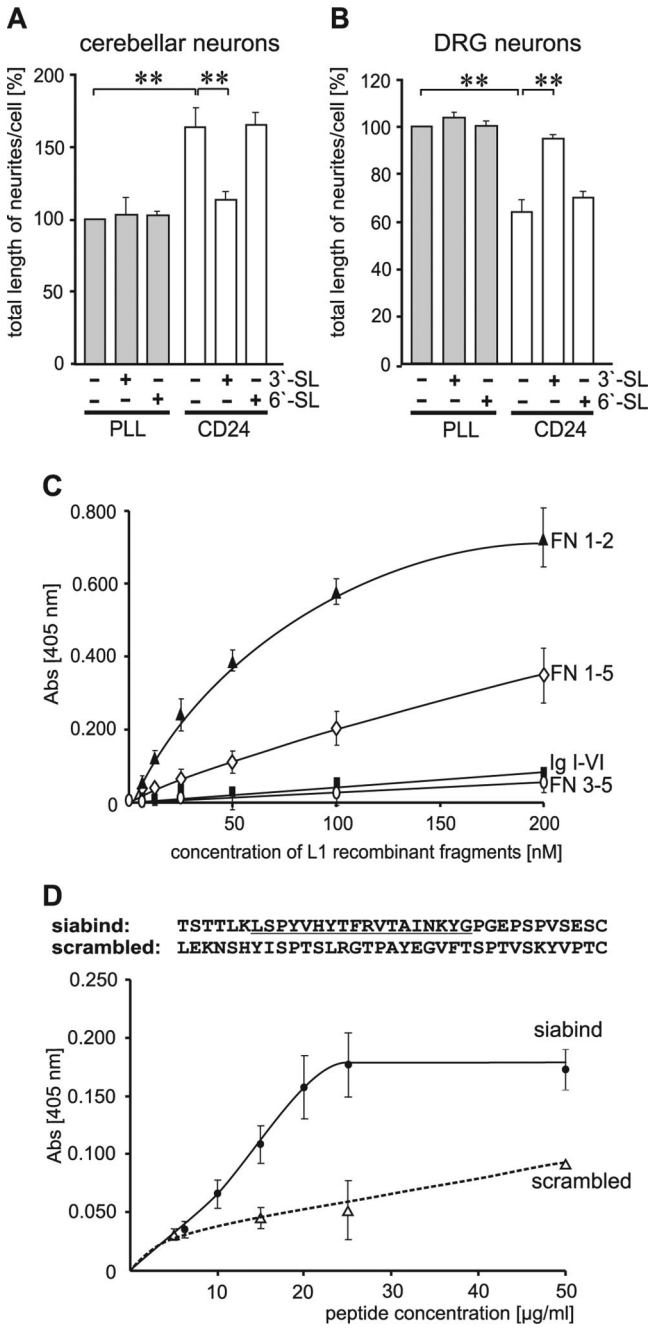

Figure 1. Sialic acid-dependent binding of L1 to CD24 affects neurite outgrowth. ***A***, ***B***, Cerebellar neurons (***A***) and DRG neurons (***B***) were grown on substrate-coated PLL or CD24 in the absence or presence of 3′-sialyl-*N*-acetyllactosamine (3′-SL) or 6′-sialyl-*N*-acetyllactosamine (6′-SL). Total length of neurites per cell was determined and shown as percentage of PLL control. Error bars indicate SD from three independent experiments. Bars marked by double asterisks ($p < 0.01$, Student's *t* test) are significantly different from the controls (PLL or CD24). ***C***, ***D***, Brain CD24 was substrate coated and incubated with different amounts of L1 fragments (***C***) and biotinylated L1-derived peptide (siabind) and its scrambled form (***D***). Amino acid sequences of peptides are shown (***D***) and underlined amino acids represent the putative sialic acid binding motif. Binding was evaluated by ELISA using L1 antibody (***C***) or streptavidin (***D***). Error bars indicate SD from at least three independent experiments. Abs, Absorbance.

Results

CD24-induced neurite outgrowth depends on α2,3-linked sialic acid

To investigate the functional role of sialic acid residues on CD24-induced neurite outgrowth (Kleene et al., 2001), α2,3-sialyl-*N*-acetyllactosamine (3′-SL) or α2,6-sialyl-*N*-acetyllactosamine (6′-SL) was applied to cerebellar or DRG neurons plated on PLL or PLL plus CD24. On CD24 substrate neurite outgrowth relative to PLL substrate was promoted in case of cerebellar neurons (Fig. 1*A*), while an inhibition was observed in case of DRG neurons (Fig. 1*B*). In the presence of 6′-SL neurite outgrowth of both neuronal cell types on CD24 was unaffected (Fig. 1*A*, *B*). How-

ever, in the presence of 3′-SL no CD24-induced promotion of neurite outgrowth from cerebellar neurons (Fig. 1*A*) and no CD24-induced inhibition of neurite outgrowth from DRG neurons (Fig. 1*B*) was observed. Thus, neurite outgrowth on substrate-coated CD24 in the presence of 3′-SL was similar to that observed on the control substrate PLL. On substrate-coated PLL, none of the glycans affected neurite outgrowth of either neuronal cell type (Fig. 1*A*,*B*).

These results indicate that CD24-induced promotion and inhibition of neurite outgrowth is specifically mediated by α2,3-linked sialic acid carried by CD24, and not by α2,6-linked sialic acid.

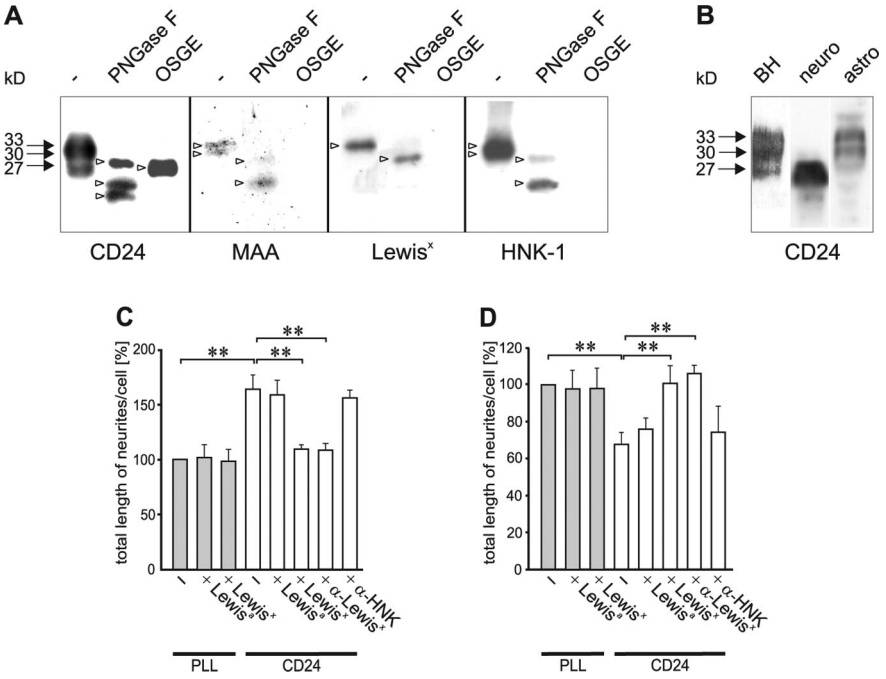

Figure 2. CD24 glycosylation pattern and effects of Lewis^x and HNK-1 glycans on CD24-induced neurite outgrowth. ***A***, Mock-treated CD24 (−), and CD24 treated with PNGase F or OSGE was subjected to Western blot analysis using CD24, Lewis^x, and HNK-1 antibodies or MAA. Arrows indicate the three CD24 glycoforms and arrowheads indicate the positions of individual bands after PNGase F, OSGE, or mock treatment. ***B***, Mouse brain homogenate (BH), cell lysates of cultured cerebellar neurons (neuro), or astrocytes (astro) were analyzed using CD24 antibody. Arrows indicate the different CD24 glycoforms. Clear bands are not always visible, as separation of highly glycosylated glycoproteins is notoriously difficult. ***C***, ***D***, Cerebellar neurons (***C***) and DRG neurons (***D***) were grown on PLL or CD24 in absence (−) or presence of Lewis^a, Lewis^x, Lewis^x antibody, or HNK-1 antibody. Total length of neurites per cell was determined and shown as percentage of PLL control. Error bars indicate SD from three independent experiments. Bars marked by double asterisks ($p < 0.01$, Student's *t* test) are significantly different from the control (PLL or CD24).

Localization and specificity of the sialic acid binding site within the L1 molecule

As the sialic acid binding protein L1 is a functional neuronal receptor for the glycosylphosphatidylinositol (GPI)-anchored molecule CD24 (Kleene et al., 2001), we wanted to identify the recognition site within the L1 molecule for the α2,3-linked sialic acid-dependent binding of CD24. Therefore, binding of recombinant proteins comprising different extracellular domains of L1 to substrate-coated CD24 purified from mouse brain was investigated by ELISA. L1 consists of six Ig-like and five fibronectin type-III homologous (FN III) domains followed by a transmembrane and a cytoplasmic domain (for review, see Brümmendorf and Rathjen, 1995). The L1 fragment carrying the first and second FN III domains showed a concentration-dependent and saturable binding to CD24, while the L1 fragment comprising the third, fourth and fifth FN III domains or comprising all six Ig-like domains did not bind to CD24 (Fig. 1*C*). Binding of the L1 fragment comprising all five FN III domains to CD24 was less efficient compared with the L1 fragment comprising only the first and second FN III domains (Fig. 1*C*), suggesting some conformational inaccessibility of the first two FN III domains in the larger construct containing all five FN III domains.

According to sequence similarities with the sialic acid binding motif of siglecs, we have proposed that the sialic binding site of L1 is present within a consensus sequence in the first FN III domain of L1 (Kleene et al., 2001). To verify this, a biotinylated synthetic peptide comprising the putative sialic acid binding site was tested by ELISA using CD24 as substrate-coat and HRP-conjugated streptavidin for detection. The peptide comprising the mouse L1 sequence spanning amino acids 678–695 that overlaps with the putative lectin consensus sequence and carries additional flanking amino acids bound to CD24 in a concentration-dependent and saturable manner, while the scrambled peptide derived from this sequence did not bind to CD24 (Fig. 1*D*). Binding of the L1 fragment comprising the first and second FN III domains to substrate-coated CD24 was reduced in the presence of α2,3-linked, but not α2,6-linked sialic acid (data not shown).

These results indicate that CD24 is recognized by a specific binding motif present in the first FN III domain of L1 and show that the binding site is specific for α2,3-linked sialic acid.

Glycosylation pattern of the different CD24 glycoforms

Next, we were interested in whether the α2,3-linked sialic acid chains are present on *O*-glycans or *N*-glycans and whether CD24 carries other functionally important carbohydrates, such as the human natural killer cell glycan HNK-1, oligomannosidic glycans or Lewis^x. CD24 purified from mouse brain was treated with *N*-glycosidase F (PNGase F) to remove *N*-glycans or with OSGE, which cleaves *O*-glycan-rich sialomucin-like glycoproteins. Western blot analysis using lectins or antibodies against carbohydrates of interest was performed to characterize the glycan pattern of CD24 before and after enzymatic treatment.

Monoclonal antibody directed against the CD24 peptide backbone detected the three major glycoforms of CD24 isolated from early postnatal mouse brain with apparent molecular weights of ~33, 30 and 27 kDa (Fig. 2*A*). After PNGase F treatment three bands of 28, 25 and 24 kDa were recognized by the CD24 antibody (Fig. 2*A*). These molecular weight shifts suggest that all three glycoforms are *N*-glycosylated. After treatment with OSGE only the 27 kDa band was recognized by the CD24 antibody (Fig. 2*A*), implying that this glycoform is resistant to OSGE and that the 30 and 33 kDa forms are *O*-glycan-rich sialoglycoproteins, which are degraded by the endopeptidase.

The lectin *Maackia amurensis* agglutinin (MAA), which is specific for α2,3-linked sialic acid, recognizes the 33 and 30 kDa glycoforms in the native CD24 sample and the corresponding 28 and 25 kDa bands in the PNGase F treated sample, while this lectin no more reacted with CD24 treated with OSGE (Fig. 2*A*). Antibody to the Lewis^x glycan recognized the 33 kDa band in the native CD24 sample and the corresponding 28 kDa band after

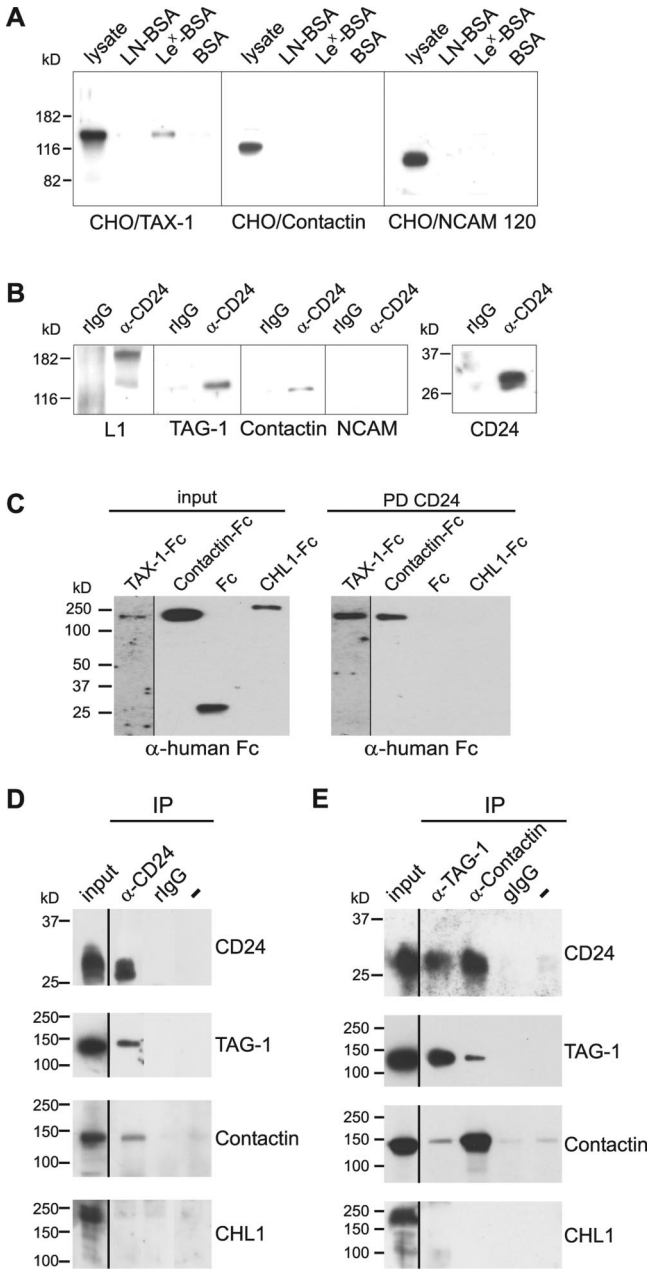

Figure 3. TAG-1 and Contactin bind to CD24 and are receptors for Lewis^x. ***A***, Lysates from CHO cells transfected with TAX-1 (CHO/TAX-1), Contactin (CHO/Contactin), or NCAM120 (CHO/NCAM120) were incubated with epoxy beads coated with Lewis^x–BSA (Le^x-BSA), *N*-acetyllactosamine–BSA (LN-BSA), and BSA. After pull-down, beads were analyzed by Western blotting using antibodies to TAG-1 (lanes 1–4), Contactin (lanes 5–8), or NCAM (lanes 9–12). ***B***, Immunoprecipitates from brain homogenate using CD24 antibody (α-CD24) or control rat IgG (rIgG) were analyzed by Western blotting using antibodies against L1, TAG-1, Contactin, NCAM, or CD24. ***C***, CD24-coupled epoxy beads were incubated with TAX-1-Fc, Contactin-Fc, CHL1-Fc, or Fc alone. After pull-down, beads (PD CD24) were analyzed by Western blotting using HRP-coupled anti-human antibody. ***D***, ***E***, Cerebellar tissue (input) was used for immunoprecipitations with CD24 with antibody (α-CD24), with control rat IgG (rIgG) or without antibody (−) or for immunoprecipitations with TAG-1 antibody (α-TAG-1), Contactin antibody (α-Contactin), or control goat IgG (gIgG) or without antibody (−). Immunoprecipitates were analyzed by Western blotting using antibodies against CD24, TAG-1, Contactin, or CHL1.

PNGase F treatment (Fig. 2*A*). The HNK-1 antibody recognized the 33 and 30 kDa glycoforms in native CD24 and the 28 and 25 kDa bands in the PNGase F treated CD24 sample (Fig. 2*A*). Neither the antibodies to Lewis^x nor to HNK-1 recognized bands after treatment of CD24 with OSGE (Fig. 2*A*). Using the lectin *Galanthus nivalis* agglutinin (GNA), which recognizes oligomannosidic structures on *N*-glycans or using antibodies specific for oligomannosides, none of the CD24 glycoforms was recognized (data not shown), indicating that CD24 does not carry detectable amounts of oligomannosidic structures.

The characterization of the glycosylation pattern of CD24 implies that the 33 kDa CD24 glycoform carries the Lewis^x epitope, the HNK-1 epitope and α2,3-linked sialic acids on *O*-glycans, while the 30 kDa glycoform carries α2,3-linked sialic acid and HNK-1 on *O*-glycans. In contrast, the 27 kDa glycoform does not carry detectable amounts of mucin-like *O*-glycans. All three major glycoforms of CD24 carry *N*-linked glycans.

Cell type-specific expression of the different CD24 glycoforms

Previous work had indicated that the 33 and 30 kDa glycoforms of CD24 are expressed by glial cells and interact in a *trans*-configuration with neuronally expressed L1, while the 27 kDa glycoform appeared to be neuron-specific and did not interact with L1 (Kleene et al., 2001). To provide experimental evidence for these suggestions we analyzed neurons and astrocytes derived from early postnatal mouse cerebella and brains, respectively, in primary cultures for expression of CD24 glycoforms by Western blotting. In early postnatal mouse brain homogenate, the three CD24 glycoforms were detectable as 33, 30 and 27 kDa bands (Fig. 2*B*). Cerebellar neurons expressed one major 27 kDa CD24 protein (Fig. 2*B*) and astrocytes expressed the 33 and 30 kDa CD24 proteins (Fig. 2*B*).

These observations imply that the 33 and 30 kDa glycoforms, which carry the α2,3-linked sialic acid, HNK-1 and Lewis^x carbohydrate structures, are expressed by astrocytes, whereas the 27 kDa glycoform devoid of these carbohydrates, and carrying yet unknown carbohydrates, is expressed by cerebellar neurons.

CD24-induced neurite outgrowth depends on Lewis^x but not on HNK-1

Since CD24 carry the functionally active Lewis^x and HNK-1 glycans, we investigated whether these structures play a role in CD24-induced neurite outgrowth. Cerebellar or DRG neurons were plated on PLL or PLL plus CD24 and maintained in the absence or presence of the Lewis^x or Lewis^a glycans or antibodies against Lewis^x or HNK-1. As observed already, CD24 substrate promoted or inhibited neurite outgrowth of cerebellar or DRG neurons, respectively (Fig. 2*C*,*D*). In the presence of the antibody against Lewis^x or Lewis^x glycan, CD24-induced promotion of neurite outgrowth was no more seen in the case of cerebellar neurons (Fig. 2*C*). Likewise, in the presence of the Lewis^x antibody or Lewis^x glycan CD24-induced inhibition of neurite outgrowth of DRG neurons was neutralized (Fig. 2*D*). As control, Lewis^a glycan did not modify the CD24-induced effects on neurite outgrowth of cerebellar or DRG neurons (Fig. 2*C*,*D*). On the PLL substrate neither carbohydrates nor antibodies affected neurite outgrowth of cerebellar or DRG neurons (Fig. 2*C*,*D*). The HNK-1 antibody did not affect neurite outgrowth either on PLL or on CD24 (Fig. 2*C*,*D*).

These results indicate that in addition to α2,3-linked sialic acid (Fig. 1) Lewis^x carried by CD24 is responsible for the CD24-mediated promotion and inhibition of neurite outgrowth, whereas HNK-1 is ineffective.

TAG-1 and Contactin are putative Lewis^x receptors

To gain insights into the structure of receptors for Lewis^x, we compared the sequences of fucose-specific (and thus Lewis^x re-

lated) plant lectins with adhesion molecules of the L1 family that are known to interact with L1. These analyses revealed significant similarities of the first Ig-like domains of Contactin and TAG-1 to several plant lectins. Other members of the L1 family did not show these similarities. Sequence homologies were observed for anti-H(O) blood group *Ulex europaeus* lectin II and *Pisum sativum* agglutinin (supplemental data, available at www.jneurosci.org; Fig. 1*A*), which have been reported to bind fucosylated oligosaccharides with high affinities (Yamamoto et al., 1992). A similarity between the four Ig-like domains of TAG-1 and Contactin with the entire sequence of the *Lotus tetragonolobus* lectin, which binds with high affinity to Lewis^x carrying glycans (Cheng et al., 1998), was also observed (supplemental data, available at www.jneurosci.org; Fig. 1*B*). TAG-1 shows a higher degree of homology with the *Lotus tetragonolobus* lectin than Contactin, in particular in two regions of high similarity (supplemental data, available at www.jneurosci.org; Fig. 1*B*).

To test whether Contactin and TAG-1 bind to Lewis^x, pull-down assays were carried out. Lewis^x or *N*-acetyllactosamine coupled to the protein carrier BSA or BSA alone were immobilized and exposed to detergent lysates of CHO cells transfected with the GPI-linked molecules TAX-1 (the human homolog of TAG-1), Contactin, or the GPI-linked form of NCAM, NCAM120. The Lewis^x–BSA conjugate pulled down TAX-1 from the corresponding cell lysate, but not Contactin or NCAM120 (Fig. 3*A*). Neither the immobilized BSA nor the *N*-acetyllactosamine–BSA conjugate pulled down TAX-1, Contactin, or NCAM120 (Fig. 3*A*).

These results indicate that TAG-1 indeed binds to Lewis^x, while a binding of Contactin to Lewis^x was not detectable under the conditions of this experiment.

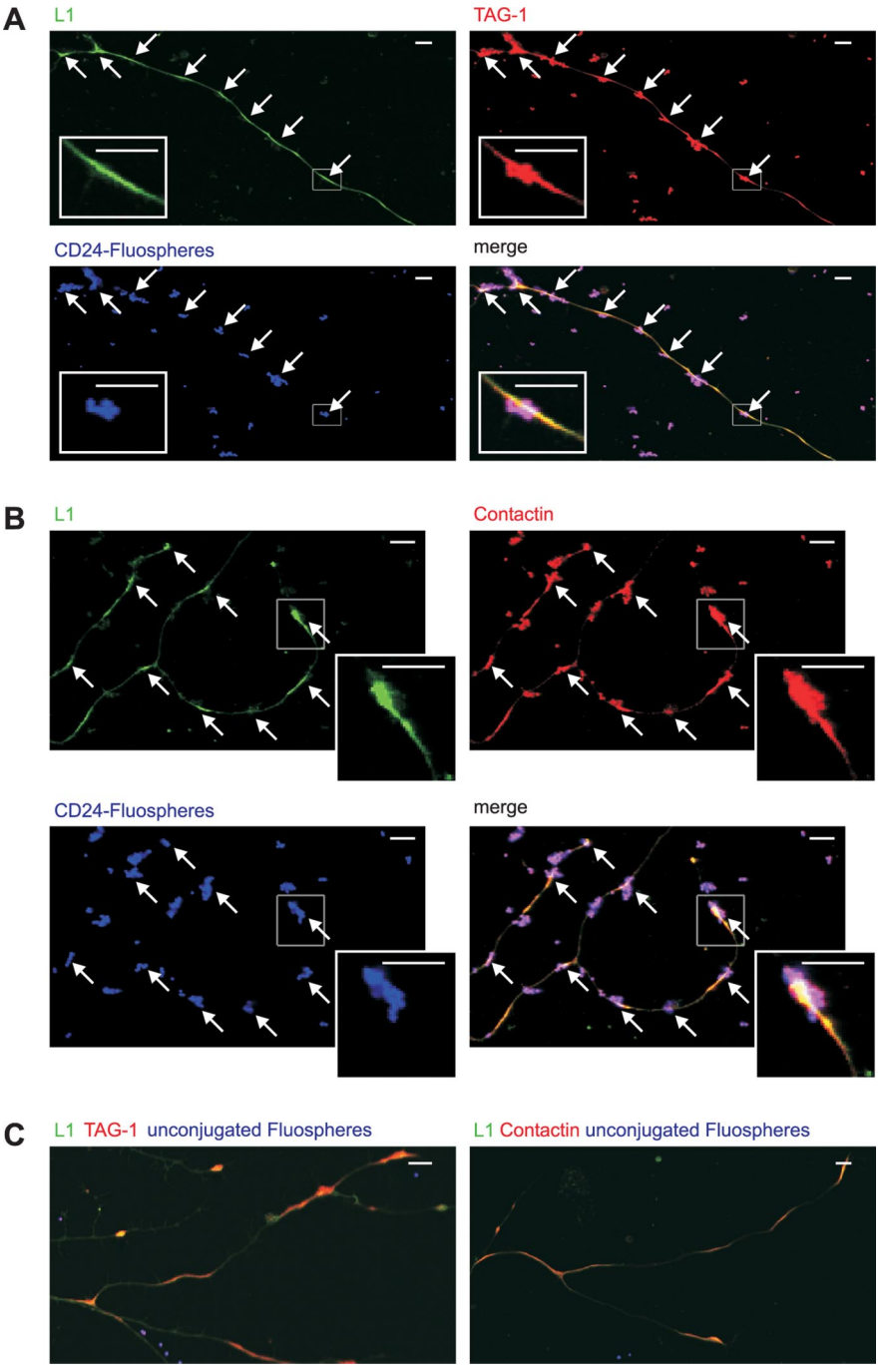

Figure 4. CD24 binds *in trans* to L1/TAG-1 or L1/Contactin clusters on cultured DRG neurons. ***A–C***, Primary cultures of wild-type DRG neurons were incubated with CD24 coated (***A***, ***B***) or unconjugated (***C***) Fluospheres and afterward immunofluorescent staining of L1 and TAG-1 (***A***, ***C***) or L1 and Contactin (***B***, ***C***) was performed. Arrows indicate clusters stained for CD24-Fluospheres, L1 and TAG-1, or Contactin. Areas in rectangles are magnified. Scale bars, 10 μm.

TAG-1 and Contactin directly interact with CD24

CD24 binds to L1, which has been shown to functionally interact with Contactin and TAG-1 (Kuhn et al., 1991; Olive et al., 1995; Buchstaller et al., 1996; Falk et al., 2002). To test whether CD24 also interacts with Contactin and TAG-1, we performed immunoprecipitations from detergent solubilized brain homogenates using monoclonal antibody against CD24. Probing the immunoprecipitates by Western blot with antibodies against L1, TAG-1, Contactin, CD24 and, as control, NCAM revealed that L1, TAG-1 and Contactin coimmunoprecipitated with CD24, while NCAM did not coimmunoprecipitate with CD24. Neither of the proteins was found in the control where a nonimmune rat IgG was used for immunoprecipitation (Fig. 3*B*). Thus, coimmunoprecipitation of TAG-1 and Contactin with CD24 indicates that these proteins interact directly or indirectly with each other.

To show a direct interaction of TAG-1 or Contactin with CD24, pull-down assays were carried out. CD24 immobilized on beads was incubated with TAX-1-Fc, Contactin-Fc and, as controls, CHL1-Fc and Fc alone. Beads coated with CD24 pulled down Contactin-Fc and TAX-1-Fc but not CHL1-Fc or Fc (Fig. 3*C*). These results show that TAX-1 and Contactin directly bind to CD24.

To further substantiate the interaction of CD24 with Contactin and TAG-1 in the cerebellum, antibodies against TAG-1,

Contactin or CD24 were used for immunoprecipitations from detergent solubilized homogenates of cerebellum. Immunoprecipitation with the CD24 antibody and probing the immunoprecipitates by Western blot analysis with antibodies against CD24, TAG-1, and Contactin revealed that TAG-1, Contactin, and CD24 immunoprecipitated with the CD24 antibody. Western blot analysis with the CHL1 antibody, as control, indicated that no CHL1 was detectable in the immunoprecipitate (Fig. 3*D*). In the control samples using nonimmune control IgG for immunoprecipitation or omitting the CD24 antibody, no CD24, TAG-1, or Contactin was detectable in the immunoprecipitates (Fig. 3*D*). Immunoprecipitations with TAG-1 or Contactin antibodies and Western blot analysis showed that Contactin, TAG-1, and CD24, but not CHL1, were coimmunoprecipitated by the TAG-1 antibody as well as by the Contactin antibody. In the absence of antibody or in the presence of nonimmune antibodies neither molecule was immunoprecipitated (Fig. 3*D*). These results indicate that the adhesion molecules CD24, TAG-1 and Contactin are associated in a protein complex in the membranes from early postnatal cerebellum.

Since it was not possible to carry out immunoprecipitation from DRGs due to the small amounts of protein derived from the tissue, the association of CD24 with L1 and Contactin or TAG-1 was analyzed in cell culture by determination of coclustering of *cis*-interacting partners on live DRG neurons with *trans*-interacting CD24. To this aim, fluorescent microspheres were coated with purified brain CD24, and these CD24-coated beads were incubated with DRG neurons followed by immunofluorescent staining of L1 and either TAG-1 or Contactin to detect colocalization. The majority of CD24-coated beads were seen in the vicinity of clusters showing of costaining of L1 and TAG-1 (Fig. 4*A*) or L1 and Contactin (Fig. 4*B*). These clusters were present along neurites in nearly constant intervals of 20–25 μm. Using unconjugated control beads no attachment of beads to the neurites was observed (Fig. 4*C*).

These results suggest that CD24 binds to complexes containing either L1 and TAG-1 or L1 and Contactin in DRG neurons.

TAG-1 and Contactin mediate CD24-induced and Lewis^x-dependent effects on neurite outgrowth of cerebellar and DRG neurons

To test whether TAG-1 and/or Contactin are involved in glycan-dependent CD24-induced neurite outgrowth, cerebellar and DRG neurons from TAG-1-deficient and Contactin-deficient mice were analyzed for neurite extension on substrate-coated CD24. Neurite outgrowth of cerebellar neurons from TAG-1- and Contactin-deficient mice was not enhanced in the presence of CD24 in contrast to neurite outgrowth of wild-type neurons that showed an increase in neurite length in the presence of CD24 (Fig. 5*A*,*B*). This effect was specific, as on the control substrate laminin, neurite outgrowth of the deficient cerebellar neurons was not changed relative to that of wild-type neurons (Fig. 5*A*,*B*). DRG neurons from TAG-1- and Contactin-deficient mice showed a significant reduction of neurite length by ~20% on the CD24 substrate relative to neurite outgrowth on PLL set to 100% (Fig. 5*C*,*D*), while a significant reduction of neurite length by ~35% was observed on the CD24 substrate relative to PLL in the case of wild-type DRG neurons (Fig. 5*C*,*D*). Since mutant neurons showed comparable neurite outgrowth as wild-type neurons on PLL, the inhibition of neurite outgrowth of TAG-1- and Contactin-deficient DRG neurons by substrate-coated CD24 was ~50% of the inhibition seen with wild-type neurons and thus represented an intermediate inhibition.

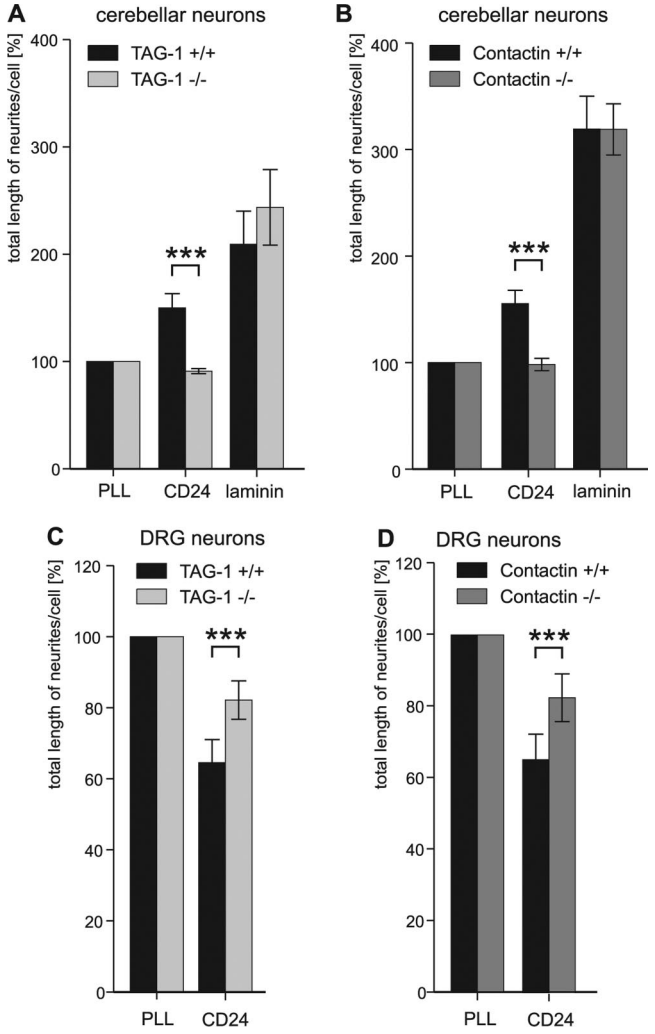

Figure 5. Involvement of TAG-1 and Contactin in CD24-induced neurite outgrowth. ***A–D***, Cerebellar (***A***, ***B***) and DRG (***C***, ***D***) neurons from TAG-1-deficient (−/−) (***A***, ***C***) or Contactin-deficient (−/−) (***B***, ***D***) and wild-type littermate (+/+) mice were grown on PLL, CD24, or laminin. Total length of neurites per cell was determined and is shown as percentage of PLL control. Error bars indicate SD from three independent experiments. Bars marked by triple asterisks ($p < 0.001$) are significantly different from the wild-type control (Student's *t* test).

The combined results imply that TAG-1 and Contactin cooperate in promoting neurite outgrowth of cerebellar neurons, since both TAG-1 and Contactin are required to mediate CD24-induced neurite outgrowth. However, TAG-1 and Contactin function individually and separately from each other in DRG neurons, since inhibition of neurite outgrowth from the deficient neurons was intermediate between maximal inhibition seen with wild-type neurons on CD24 and no inhibition seen with DRG neurons on PLL. Intermediate inhibition could be mediated by Contactin in TAG-1-deficient neurons and by TAG-1 in Contactin-deficient neurons.

To test this assumption, we performed neurite outgrowth experiments of TAG-1-deficient and Contactin-deficient DRG neurons in the presence of either antibodies to Contactin or TAG-1. In the presence of Contactin antibody, but not of TAG-1 antibody, the intermediate inhibition of neurite outgrowth of TAG-1-deficient DRG neurons on the CD24 substrate was abolished and neurite outgrowth was similar to that observed on the PLL substrate (Fig. 6*A*). Similarly, intermediate inhibition of neurite outgrowth of Contactin-deficient DRG neurons on CD24

substrate was neutralized by application of TAG-1 antibody, but not Contactin antibody (Fig. 6*B*). When compared with the inhibition seen in the absence of antibodies, wild-type DRG neurons showed intermediate inhibition of neurite outgrowth on CD24 in the presence of either TAG-1 antibody or Contactin antibody (Fig. 6*C*). This intermediate inhibition of neurite outgrowth resembles the CD24-induced intermediate inhibition of neurite outgrowth of TAG-1- or Contactin-deficient DRG neurons. Application of both antibodies completely abolished the inhibition of neurite outgrowth of wild-type DRG neurons on CD24 and resulted in neurite outgrowth which was similar to that seen on PLL (Fig. 6*C*). None of the antibodies showed any effect on neurite outgrowth of DRG neurons when grown on PLL like shown exemplarily in Figure 6*C* for the wild-type DRG neurons. Additionally, higher concentrations of individual antibodies did not completely abolish the inhibition, excluding concentration dependency of the antibody effects (data not shown).

These results support the view that the CD24-induced intermediate inhibition of neurite outgrowth of TAG-1-deficient DRG neurons is mediated by Contactin, while TAG-1 mediates the CD24-induced intermediate inhibition of neurite outgrowth of Contactin-deficient DRG neurons.

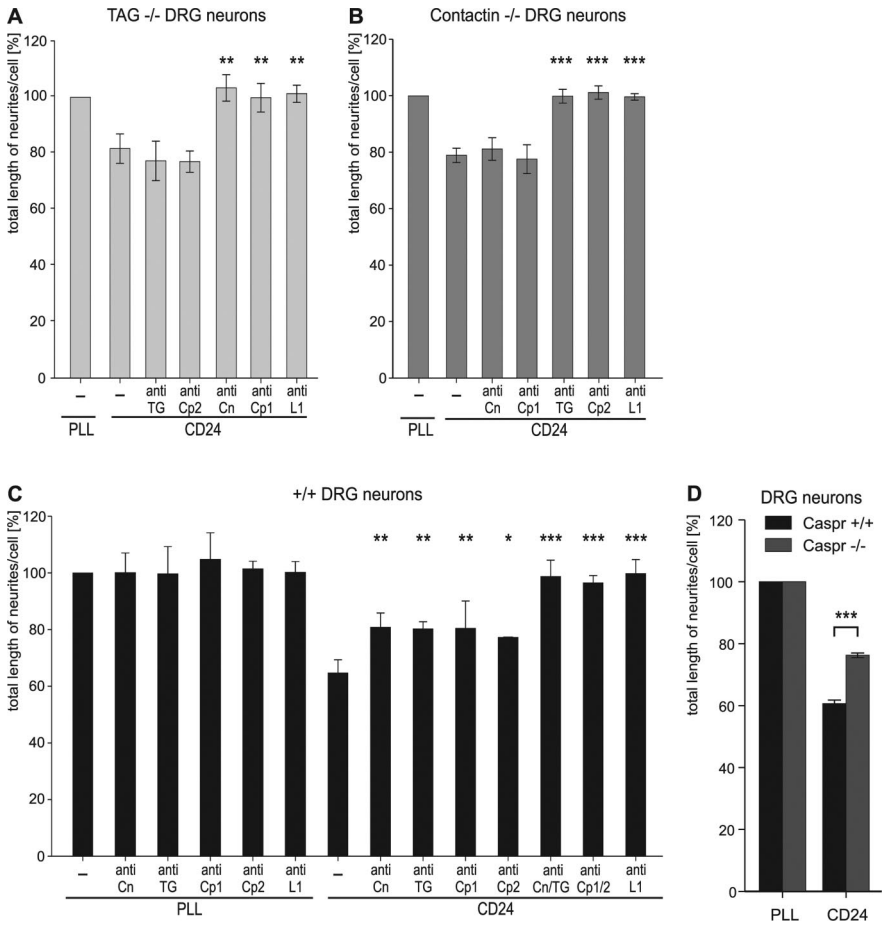

Figure 6. Synergistic effects of TAG-1/Caspr2 and Contactin/Caspr in CD24-mediated neurite outgrowth of DRG neurons. ***A–D***, DRG neurons from TAG-1-deficient (−/−) (***A***), Contactin-deficient (−/−) (***B***), and wild-type littermate (+/+) (***C***) mice or DRG neurons from Caspr1-deficient (−/−) and wild-type littermate (+/+) mice (***D***) were grown on PLL or CD24 in the absence or presence of antibodies against TAG-1 (TG), Contactin (Cn), Caspr1 (Cp1), Caspr2 (Cp2), or L1 (***A–C***). Total length of neurites per cell was determined and is shown as percentage of PLL control. Error bars indicate SD from three independent experiments. Bars marked by single asterisks ($p < 0.05$), double asterisks ($p < 0.01$), and triple asterisks ($p < 0.001$) are significantly different from the wild-type control (Student's *t* test). ***A–C***, Values for PLL were not affected by any antibody, as exemplified in ***C***.

Interactions of Contactin with Caspr1 and TAG-1 with Caspr2 mediate the CD24-induced inhibition of neurite outgrowth of DRG neurons

Since the GPI-anchored molecules Contactin and TAG-1 cannot function as transmembrane signal transducers that trigger CD24-induced responses leading to neurite outgrowth, it was very likely that transmembrane *cis*-interacting proteins of Contactin and TAG-1 mediate the CD24-induced effects on neurite outgrowth. Caspr1 is a binding partner of Contactin (Faivre-Sarrailh et al., 2000; Bonnon et al., 2003) and Caspr2 is a binding partner of TAG-1 (Poliak et al., 2003; Traka et al., 2003; Tzimourakas et al., 2007).

Immunoprecipitation from homogenates of cerebellum using a CD24 antibody showed a coimmunoprecipitation of Contactin and TAG-1 (Fig. 3*D*), but coimmunoprecipitation of Caspr1 and Caspr2 with CD24 was not detectable (data not shown), suggesting that neither Caspr1 nor Caspr2 are involved in CD24-induced neurite outgrowth of cerebellar neurons.

By immunostaining of cultured DRG neurons, we tested whether Caspr1 or Caspr2 colocalized with Contactin and L1 or with TAG-1 and L1, respectively. Staining of Caspr1 and Caspr2 was observed in clusters and the staining overlapped with that of L1 (Fig. 7*A*,*B*), indicating that both Caspr1 and Caspr2 were expressed in DRG neurons in a pattern similar to Contactin and TAG-1. These results indicate that in DRG neurons Caspr1 and Caspr2 are *cis*-interacting partners of L1 and Contactin or TAG-1, respectively, and suggest that they are involved in CD24-induced neurite outgrowth of DRG neurons.

To test whether Caspr1 and Caspr2 play a role in CD24-induced neurite outgrowth polyclonal antibodies directed against the extracellular domain of Caspr1 or Caspr2 were applied to cerebellar and DRG neurons. In the presence of either antibody neurite outgrowth of cerebellar neurons on the CD24 and PLL substrate was not affected (data not shown), indicating that neither Caspr1 nor Caspr2 acted as Contactin and TAG-1 associated signal transducers mediating CD24-induced neurite outgrowth. The intermediate inhibition of neurite outgrowth of TAG-deficient DRG neurons on the CD24 substrate was abolished in the presence of the Caspr1 antibody, but not the Caspr2 antibody (Fig. 6*A*). However, intermediate inhibition of neurite outgrowth of Contactin-deficient DRG neurons on the CD24 substrate was abrogated in the presence of Caspr2, but not Caspr1 antibody (Fig. 6*B*). Application of either antibody to wild-type DRG neurons revealed intermediate inhibition of neurite outgrowth on the CD24 substrate (Fig. 6*C*). This inhibition was similar to that observed with Contactin- or TAG-1-deficient DRG neurons without antibodies. Application of both antibodies together completely abolished the CD24-induced inhibition of neurite outgrowth of wild-type DRG neurons (Fig. 6*C*). None of

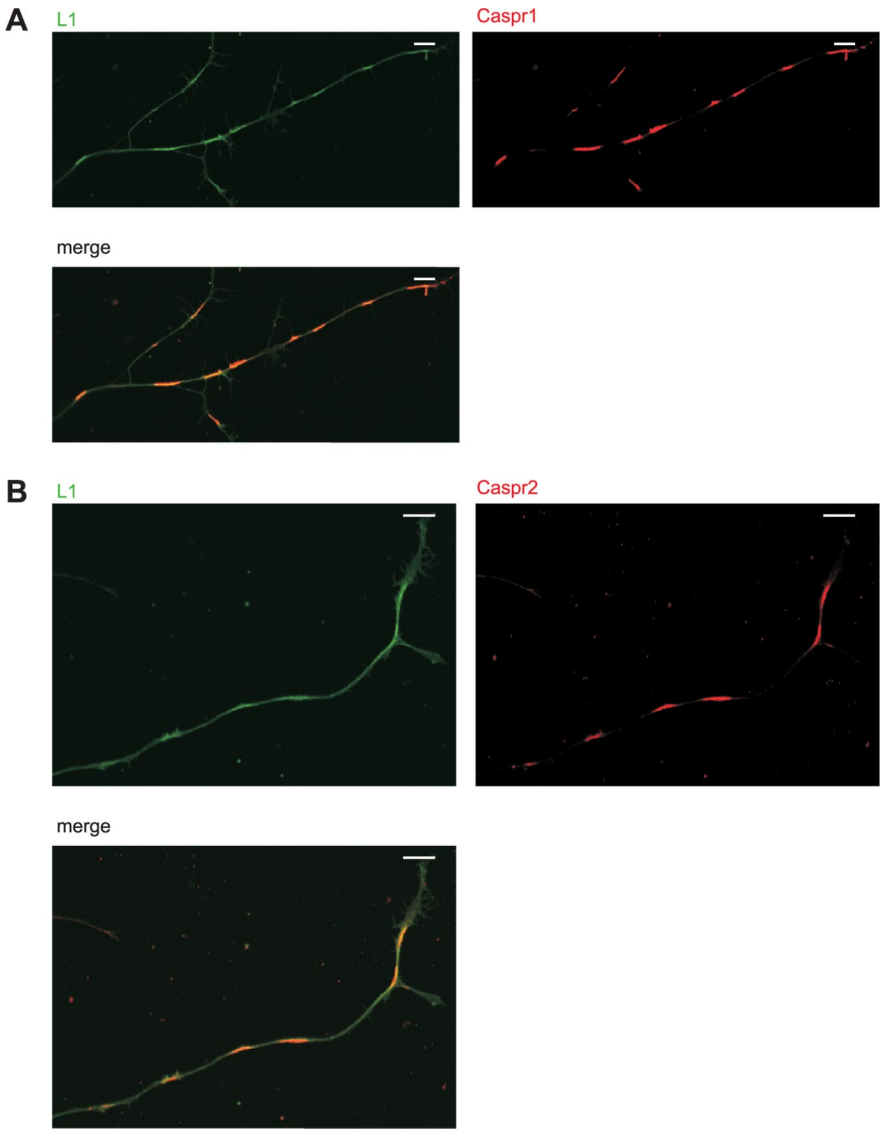

Figure 7. Caspr1 and Caspr2 colocalize with L1 on cultured DRG neurons. ***A***, ***B***, DRG neurons grown on PLL were labeled by immunofluorescence using antibodies to L1 and Caspr1 (***A***) or L1 and Caspr2 (***B***). Scale bars, 10 μm.

the antibodies showed any effect on neurite outgrowth of either DRG neurons when grown on PLL like shown in Figure 6*C* for the wild-type DRG neurons. These results show that the CD24 triggered signals via Contactin are mediated by Caspr1, while those triggered by TAG-1 depend on Caspr2. To further confirm that Caspr1 is involved in CD24-induced inhibition of neurite outgrowth of DRG neurons we used DRG neurons from Caspr1-deficient mice. On CD24 an intermediate inhibition of neurite outgrowth of Caspr1-deficient DRG neurons was observed (Fig. 6*D*), being similar to that observed with Contactin-deficient DRG neurons (Fig. 5*D*).

These results strongly suggest that the CD24 triggered signals via Contactin are transduced by Caspr1, while those triggered by TAG-1 depend on Caspr2. Since we did not have access to Caspr2-deficient mice, we could not do a similar analysis.

L1 has been shown to be necessary for CD24-mediated inhibition of DRG neurons (Kleene et al., 2001). To analyze whether the Contactin/Caspr1- and TAG-1/Caspr2-mediated neurite outgrowth induced by CD24 requires L1, DRG neurons from wild-type as well as TAG-1 and Contactin-deficient mice were grown on CD24 as a substrate in the presence of an antibody directed against the extracellular domain of L1. In all cases the inhibitory effect of CD24 on neurite outgrowth was abolished in the presence of L1 antibody (Fig. 6*A–C*) indicating that both the TAG-1/Caspr2- and Contactin/Caspr1-mediated effects of CD24 on neurite outgrowth of DRG neurons depend on L1.

Finally, we investigated whether the intermediate inhibition of neurite outgrowth of TAG-1- or Contactin-deficient DRG neurons on the CD24 substrate was Lewis^x-dependent by applying the Lewis^x and, as control, the Lewis^a glycan to the cultures. In the presence of Lewis^x but not Lewis^a glycans the intermediate inhibition of neurite outgrowth of Contactin- as well as of TAG-1-deficient DRG neurons was abolished, being similar to the neurite outgrowth on PLL as substrate (Fig. 8*A*, *B*). Neither glycans showed any effect on neurite outgrowth on the PLL substrate as neurite lengths were comparable to the controls in Figure 2, *C* and *D*.

The results indicate that the intermediate neurite outgrowth of DRG neurons from both Contactin- and TAG-1-deficient mice is Lewis^x–dependent. They furthermore suggest that TAG-1 and Contactin function independently as Lewis^x receptors on DRG neurons and mediate the Lewis^x-dependent CD24-induced inhibition of neurite outgrowth.

CD24-deficient mice recover less after spinal cord injury compared with wild-type littermates

To analyze the importance of CD24 in neurite outgrowth, in particular in axonal growth, *in vivo*, we compared the motor recovery after lower thoracic spinal cord compression in CD24-deficient mice and their wild-type littermates. Spinal cord injury caused severe disabilities in both CD24-deficient and wild-type mice, as assessed by the BMS 1 week after injury (Fig. 9*A*). Between one and 6 weeks after injury, locomotor function improved in both genotypes, but improvement was better in wild-type littermates than in CD24-deficient mice, not only estimated by BMS evaluation, but also by measurement of foot stepping angle (Fig. 9*B*). Foot-stepping angle describes the plantar stepping ability and was shown to correlate well with the BMS score (Apostolova et al., 2006). Rump-height index and extension-flexion ratio measure the ability of lower limbs to support body weight and to perform voluntary movements without weight support, respectively. The recovery of these functions was very poor in spinal cord injured mice regardless of genotype (Fig. 9*C*,*D*). Numbers of correct steps made by the animals during inclined ladder climbing, reduced to approximately zero in both genotypes 1 week after injury, did not improve with time in injured mice either (data not shown). These results indicate a severe degree of injury in both groups of mice, but at this injury level

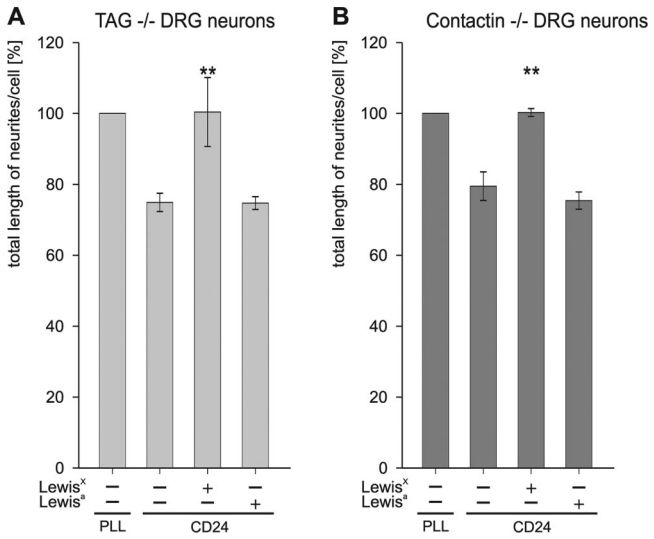

Figure 8. Lewis^x-dependent effects of TAG-1 and Contactin in CD24-mediated neurite outgrowth of DRG neurons. ***A***, ***B***, DRG neurons from TAG-1-deficient (−/−) (***A***) and Contactin-deficient (−/−) (***B***) mice were grown on PLL or CD24 in the absence or presence of Lewis^a or Lewis^x. Total length of neurites per cell was determined and is shown as percentage of PLL control. Error bars indicate SD from three independent experiments. Bars marked by double asterisks ($p < 0.01$) are significantly different from the wild-type control (Student's *t* test). Values for PLL were not affected by any glycan, as exemplified in Figure 2*D*.

there is a worse outcome in CD24-deficient mice compared with their wild-type littermates.

Next, we looked for histological evidence for the reduced locomotor recovery associated with CD24 deficiency. We stained longitudinal sections of spinal cords 6 weeks after injury with antibodies against tyrosine hydroxylase (TH) to label catecholaminergic (dopaminergic and noradrenergic) axons, previously shown to be important for ground locomotion (Jakovcevski et al., 2007). We also used an antibody against neurofilament, which labels all spinal cord axons. With both antibodies we observed enhanced sprouting of axons at the lesion site of wild-type compared with CD24-deficient spinal cords (Fig. 9*E*,*F*). We also counted numbers of TH positive and neurofilament positive axons beyond an arbitrarily selected border 250 μm caudal to the lesion site at 6 weeks after injury, with more axons having regrown in wild-type versus CD24-deficient mice (Fig. 9*G*). The decreased number of axonal fibers caudally to the lesion site, either representing axons that have grown through the lesion site or newly formed branches of the spared axons, suggests an abnormally low regenerative capacity of axons in the injured spinal cord of CD24-deficient mice.

These results show that CD24 plays an important role in enhancing axon regrowth and thus in neurite outgrowth *in vivo*.

CD24 influences neurite outgrowth of several neuronal cell types in a similar manner

CD24 is known to promote neurite outgrowth of cerebellar neurons and to inhibit that of DRG neurons and postnatal retinal ganglion cells both in substrate coated cultures and in cocultures with CD24-transfected astrocytoma cells (Shewan et al., 1996; Kleene et al., 2001). To gain further insights into the role of CD24 in mediating neurite outgrowth, we investigated CD24-dependency of neurite outgrowth from other types of neurons, namely of primary cultured wild-type neurons from hippocampus, spinal cord and cortex. Hippocampal neurons showed a significant increase in neurite length in the presence of CD24 by ~45% compared with PLL set to 100% (Fig. 10*A*). The majority of spinal cord and cortical neurons also showed enhanced neurite outgrowth of ~45% and 70%, respectively, on CD24 relative to PLL (Fig. 10*B*,*C*). In contrast, neurite lengths of the smaller populations of large-sized motoneurons present in primary cultures of spinal cord and cortical neurons was significantly reduced by ~35% on the CD24 substrate relative to neurite lengths on control substrates (Fig. 10*B*,*C*).

These results show that CD24 promotes neurite outgrowth of hippocampal neurons and of spinal cord and cortical non-motoneurons, and it promotes neurite outgrowth of cerebellar neurons. In contrast, CD24 inhibits outgrowth of motoneurons from spinal cord and from cortex comparable to inhibition of neurite outgrowth from DRG neurons or retinal ganglion cells.

Discussion

L1 is a neuronal receptor for α2,3-linked sialic acid on CD24, while TAG-1 and Contactin are neuronal receptors for Lewis^x on CD24

In previous studies, we have shown that CD24-mediated neurite outgrowth of cerebellar and DRG neurons requires L1 at the neuronal surface and depends on sialic acid residues carried by CD24 (Kleene et al., 2001). In the present study, we identified the binding site for sialic acid within the first FN III domain of L1. L1 bound sialic acid preferably in α2,3 linkage and barely in α2,6 linkage. Furthermore, α2,3-linked but not α2,6-linked sialyl residues were functionally active in mediating CD24-induced effects on neurite outgrowth of cerebellar and DRG neurons. In addition to α2,3-linked sialic acid the Lewis^x glycan also mediates CD24-dependent neurite outgrowth of cerebellar and DRG neurons. TAG-1 and Contactin were identified as the neuronal receptors for the Lewis^x glycans and mediate Lewis^x-dependent neurite outgrowth.

α2,3-Linked sialic acids were identified on *O*-glycans of the 30 and 33 kDa CD24 glycoforms present on cultured astrocytes, but not on cultured neurons. The 33 kDa glycoform of CD24 carries also Lewis^x and HNK-1 epitopes on *O*-glycans.

Both α2,3-linked sialic acid and Lewis^x on glycans carried by CD24 are required to modulate CD24-induced neurite outgrowth

The observation that both α2,3-linked sialic acid and Lewis^x glycans are required for CD24-induced modulation of neurite outgrowth suggested a functional coupling of signal transduction pathways triggered in neurons by α2,3-linked sialic acid- and Lewis^x-carrying carbohydrates present on glial CD24 glycoforms. The presence of both carbohydrates, possibly on one CD24 molecule, contributes to a glia–neuron interaction. Disruption of binding of the α2,3-sialyl or Lewis^x glycans to their corresponding neuronal receptors by removal of sialic acids from CD24 (Kleene et al., 2001), by applying Lewis^x antibody or by addition of soluble Lewis^x or α2,3-linked sialic acid carrying carbohydrates abolished the glycan-dependent effects on neurite outgrowth. In addition, CD24-induced effects on neurite outgrowth of neurons deficient in L1 as the α2,3-linked sialic acid receptor (Kleene et al., 2001) or deficient in TAG-1 or Contactin as the Lewis^x receptors were abolished. Similarly, blocking antibodies against L1, Contactin and TAG-1 interfered with the function of L1, Contactin, and TAG-1 as neuronal receptors for CD24. These results indicate that neither Lewis^x nor α2,3-linked sialic acids alone are able to modulate CD24-dependent neurite outgrowth and both glycans and their corresponding neuronal receptors are re-

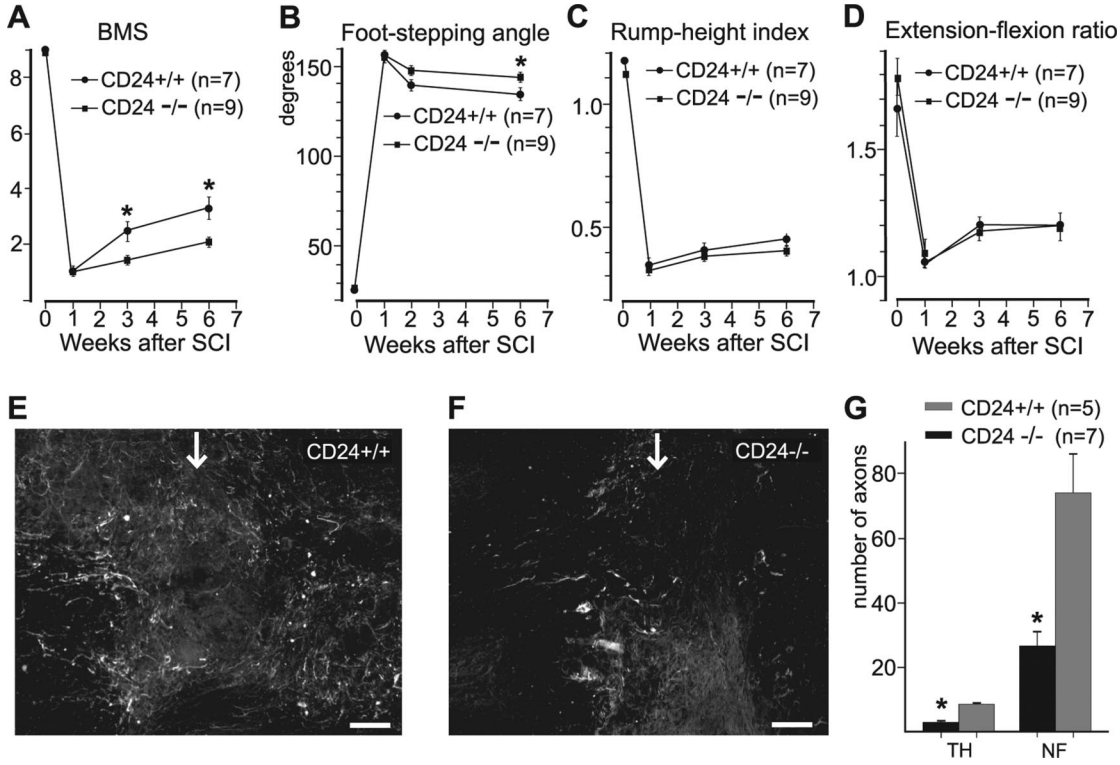

Figure 9. Regeneration after spinal cord injury in CD24 $^{+/+}$ and CD24 $^{-/-}$ mice. ***A–D***, Time course and degree of functional recovery in CD24 $^{-/-}$ mice and CD24 $^{+/+}$ littermates after spinal cord injury. Shown are mean values ± SEM of open-field locomotion (BMS) scores (***A***), foot-stepping angles (***B***), rump-height indices (***C***), and extension-flexion ratios (***D***) before surgery (day 0) and at 1, 3, and 6 weeks after injury. Numbers of animals are given in parentheses; asterisks indicate significant differences between group mean values at a given time point ($p < 0.05$, one-way ANOVA for repeated measurements with Tukey *post hoc* test). ***E***, ***F***, Representative images of immunofluorescent stainings for neurofilament at the lesion epicenter (arrow) in CD24 $^{+/+}$ littermate (***E***) and CD24 $^{-/-}$ (***F***) mice. Left is rostral, right is caudal. ***G***, Mean numbers of TH-positive and NF-positive fibers crossing an arbitrary border 250 μm caudally from the lesion site at 6 weeks after the lesion (*$p < 0.05$; Wilcoxon–Mann–Whitney test).

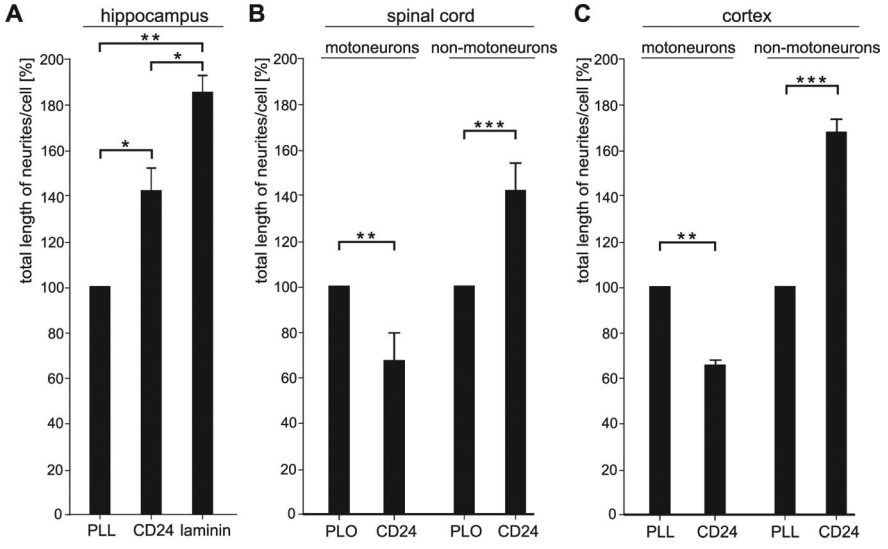

Figure 10. CD24-mediated neurite outgrowth of hippocampal, cortical, and spinal cord neurons. ***A***, Hippocampal neurons from wild-type mice were grown on PLL, CD24, or laminin. ***B***, Wild-type spinal cord neurons were grown on PLO or CD24. The culture contains round non-motoneurons with a diameter of ~10 μm and motoneurons having a large triangular cell body with an edge length of 15–20 μm. ***C***, Wild-type cortical neurons were grown on PLL or CD24. The culture contains non-motoneurons and motoneurons. ***A–C***, Total length of neurites per cell was determined and is shown as percentage of the PLL or PLO controls. Error bars indicate SD from three independent experiments. Bars marked by asterisks ($p < 0.05$) or double asterisks ($p < 0.01$) are significantly different from the control (PLL, PLO, or laminin; Student's *t* test).

quired for carbohydrate-dependent stimulation of neurite outgrowth of cerebellar neurons or inhibition of outgrowth of DRG neurons by CD24. We thus provide evidence for the role of glycans in mediating and modulating glia–neuron interactions. However, it is possible that these glycans also mediate neuron–neuron or glia–glia interactions.

Heterophilic interaction of L1 with TAG-1 and Contactin

A functional heterophilic interaction of L1 with TAG-1 has been shown by colocalization on DRG neurons (Kuhn et al., 1991) and coimmunoprecipitation from cells cotransfected with the two molecules (Kunz et al., 1998; Malhotra et al., 1998) or from DRG neurons (Buchstaller et al., 1996). Other reports have also documented an interaction of Contactin and L1 (Brümmendorf et al., 1993; Olive et al., 1995). The sites involved in heterophilic interaction of L1 with TAG-1 have been mapped to the four Ig-like domains of TAG-1 (Rader et al., 1996; Malhotra et al., 1998) and the four Ig-like domains of Contactin have been shown to mediate neurite outgrowth (Brümmendorf et al., 1993). Interestingly, these sites coincide with the proposed binding sites for Lewis^x within TAG-1 and Contactin. However, it is still not known whether the heterophilic interactions between L1 and TAG-1 or Contactin are mediated by direct protein–protein interactions or whether carbohydrates are involved. Although we only provide evidence for the involvement

of glycans in heterophilic *trans* interactions of L1, TAG-1 and/or Contactin with CD24, we cannot exclude that heterophilic *cis* interactions are also influenced by glycans.

Roles of TAG-1 and Contactin as coreceptors in L1-mediated carbohydrate-dependent neurite outgrowth

We have shown that TAG-1 and Contactin are neuronal receptors for Lewis^x carrying glycans on glial CD24 glycoforms, while L1 is the neuronal receptor for α2,3-linked sialic acids on these CD24 glycoforms. In the cerebellum, TAG-1 and Contactin are present in a complex together with L1 as indicated by coimmunoprecipitation. Accordingly, α2,3-linked sialic acid and Lewis^x glycans of glial CD24 mediate the heterophilic *trans* interaction with the neuronal *cis*-interacting L1, TAG-1 and Contactin molecules (Fig. 11) leading to signal transduction events that stimulate neurite outgrowth. So far it is not known which of these proteins directly interact and if there are other cell adhesion molecules involved in this process.

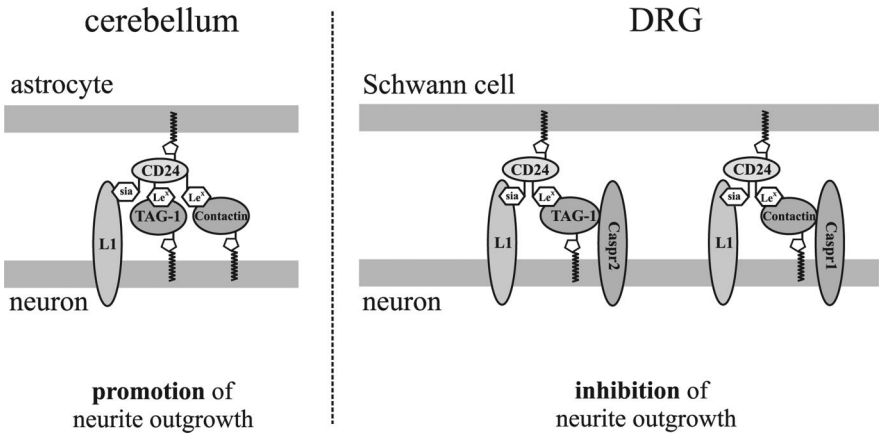

Figure 11. Scheme of a working model: role of Lewis^x and α2,3-linked sialic acid in modulating glia–neuron interactions. L1 on neurons binds to α2,3-linked sialic acid carried by glia-derived CD24, and neuronal TAG-1 and Contactin bind to Lewis^x carried by glia-derived CD24. In the case of cerebellar neurons, a complex formed by neuronal L1, TAG-1, and Contactin leads to signal transduction promoting neurite outgrowth. Inhibition of neurite outgrowth in DRG neurons is induced by two independent complexes of either L1, TAG-1, and Caspr2 or L1, Contactin, and Caspr1.

We showed that CD24-mediated neurite outgrowth of cerebellar neurons depends on Contactin and TAG-1, but is independent of their binding partners Caspr1 and Caspr2. This notion is supported by findings that Contactin acts independently of Caspr1 in cerebellar morphogenesis, such as parallel fiber orientation: while orientation of parallel fibers in the cerebellar molecular layer is impaired in Contactin-deficient mice (Berglund et al., 1999; Boyle et al., 2001), this feature is unaffected in Caspr1-deficient mice (Pillai et al., 2007).

In DRG neurons, α2,3-sialyl residues and Lewis^x on CD24 trigger an interaction either between L1, TAG-1 and Caspr2 or between L1, Contactin, and Caspr1. Our results indicate that the CD24-induced glycan-dependent functional coupling of Contactin and its *cis*-interacting partner Caspr1 (Faivre-Sarrailh et al., 2000; Bonnon et al., 2003) with L1 inhibits neurite outgrowth of DRG neurons. Similarly, the coupling of TAG-1 and its *cis*-interacting partner Caspr2 (Poliak et al., 2003) with L1 also inhibits neurite outgrowth of DRG neurons. Thus, both Caspr1 and Caspr2 exert inhibitory functions on neurite outgrowth of DRG neurons (Fig. 11). It is interesting in this respect that Caspr1 and Contactin are involved in the organization of the paranodal septate junction of myelinated axons (Rios et al., 2000; Salzer, 2003), while the association between Caspr2 and TAG-1 is essential for the organization of the juxtaparanodal regions of myelinating axons (Poliak et al., 2003; Traka et al., 2003). Paranodes and juxtaparanodes are specialized membrane subdomains and possess distinct compositions in ion channels and cell adhesion molecules (Salzer, 2003). The juxtaparanodal region and the paranodal junction are involved in the organization of the node of Ranvier, which plays a crucial role in the generation and rapid propagation of action potentials in myelinated axons. The specialized cellular subdomains at the node of Ranvier are formed through multiple contacts between the axonal and glial membranes. Deficiency in either Caspr1 or Contactin results in the disorganization of the paranodal loops and a reduction in nerve conduction velocity (Bhat et al., 2001; Boyle et al., 2001), while deficiency of Caspr2 and TAG-1 showed no alterations in the electrophysiological properties of peripheral nerves, although the enrichment of K^+ channels at the juxtanodal region was severely disrupted (Poliak et al., 2003; Traka et al., 2003). In the case of DRG neurons, it is conceivable that glycans on CD24 present on Schwann cells or astrocytes and their receptors L1, Contactin, or TAG-1 on axons mediate the formation of cell contacts between glial and neuronal cells and/or foster *cis* interactions between L1, TAG-1, and Caspr2 or between L1, Contactin, and Caspr1 (Fig. 11). These interactions may trigger signal transduction pathways leading to the inhibition of neurite outgrowth and thereby allowing the initiation of the formation of paranodes and juxtaparanodes. It is striking that CD24 binds to clusters of L1 and TAG-1 or L1 and Contactin that occur with regular intervals. That these may represent preformed sites for directed subsequent glial ensheathment preceding myelination is very tempting to speculate. As neurite outgrowth mediated by CD24 *in vivo* occurs before the onset of myelination, it is likely that glia-derived CD24 binds to receptors at the neuronal cell surface. Whether CD24 forms protein complexes at nodes of Ranvier and colocalizes with such protein is presently not possible to determine because of the difficulties to obtain clear immunohistological images with the presently available antibodies. It is, however, tempting to speculate that glycans and their receptors contribute to the formation and maintenance of complex structures in dependence on the glycan composition of the interacting adhesion molecules. Interestingly, the glycosylation pattern of Contactin regulates its binding to Caspr1 (Bonnon et al., 2007); only Contactin carrying mannose-rich *N*-glycans associates with Caspr1 and neurofascin-155, which is the glial binding partner of Contactin at paranodes, whereas Contactin which carries complex *N*-glycans is not associated with Caspr1 and does not interact with neurofascin-155.

As CD24 promotes neurite outgrowth of cerebellar and hippocampal neurons as well as non-motoneurons from spinal cord and cortex, but inhibits outgrowth of DRG neurons, retinal ganglion cells and motoneurons, the neuronal receptors must be different between the neuronal cell types that show enhanced versus reduced neurite outgrowth. Both cerebellar and hippocampal granule cells consist of mainly unmyelinated neurons, whereas axons from retinal ganglion cells, DRG neurons and motoneurons are ensheathed by oligodendrocytes or Schwann cells. Thus, these different properties generate functional differ-

ences in CD24 mediated neurite outgrowth. Our observations on axonal regeneration and functional recovery after spinal cord injury provide evidence that CD24 is also involved in neurite outgrowth *in vivo*. Although it would be difficult to assess contribution of each individual axonal pathway to functional recovery, our data suggest that CD24 has an overall enhancing impact on regeneration after injury.

It will be important to investigate how glia-derived CD24 interdigitates in the network of glycans and their receptors at axonal cell surfaces in the central and peripheral nervous systems and how this network induces specific signal transduction pathways in the subsequently functionally specialized nodal subdomains, in particular with a view on the mechanisms of neuron–glia interactions not only in normal development and structural maintenance in the adult, but also in demyelinating diseases.

References

Apostolova I, Irintchev A, Schachner M (2006) Tenascin-R restricts posttraumatic remodeling of motoneuron innervation and functional recovery after spinal cord injury in adult mice. J Neurosci 26:7849–7859.

Appel F, Holm J, Conscience JF, Schachner M (1993) Several extracellular domains of the neural cell adhesion molecule L1 are involved in neurite outgrowth and cell body adhesion. J Neurosci 13:4764–4775.

Basso DM, Fisher LC, Anderson AJ, Jakeman LB, McTigue DM, Popovich PG (2006) Basso Mouse Scale for locomotion detects differences in recovery after spinal cord injury in five common mouse strains. J Neurotrauma 23:635–659.

Berglund EO, Murai KK, Fredette B, Sekerková G, Marturano B, Weber L, Mugnaini E, Ranscht B (1999) Ataxia and abnormal cerebellar microorganization in mice with ablated Contactin gene expression. Neuron 24:739–750.

Bhat MA, Rios JC, Lu Y, Garcia-Fresco GP, Ching W, St Martin M, Li J, Einheber S, Chesler M, Rosenbluth J, Salzer JL, Bellen HJ (2001) Axon-glia interactions and the domain organization of myelinated axons requires neurexin IV/Caspr/Paranodin. Neuron 30:369–383.

Bonnon C, Goutebroze L, Denisenko-Nehrbass N, Girault JA, Faivre-Sarrailh C (2003) The paranodal complex of F3/contactin and caspr/paranodin traffics to the cell surface via a non-conventional pathway. J Biol Chem 278:48339–48347.

Bonnon C, Bel C, Goutebroze L, Maigret B, Girault JA, Faivre-Sarrailh C (2007) PGY repeats and N-glycans govern the trafficking of paranodin and its selective association with contactin and neurofascin-155. Mol Biol Cell 18:229–241.

Boyle ME, Berglund EO, Murai KK, Weber L, Peles E, Ranscht B (2001) Contactin orchestrates assembly of the septate-like junctions at the paranode in myelinated peripheral nerve. Neuron 30:385–397.

Brito C, Escrevente C, Reis CA, Lee VM, Trojanowski JQ, Costa J (2007) Increased levels of fucosyltransferase IX and carbohydrate Lewis(x) adhesion determinant in human NT2N neurons. J Neurosci Res 85:1260–1270.

Brümmendorf T, Rathjen FG (1995) Cell adhesion molecules 1: immunoglobulin superfamily. Protein Profile 2:963–1108.

Brümmendorf T, Hubert M, Treubert U, Leuschner R, Tárnok A, Rathjen FG (1993) The axonal recognition molecule F11 is a multifunctional protein: specific domains mediate interactions with Ng-CAM and restricin. Neuron 10:711–727.

Buchstaller A, Kunz S, Berger P, Kunz B, Ziegler U, Rader C, Sonderegger P (1996) Cell adhesion molecules NgCAM and axonin-1 form heterodimers in the neuronal membrane and cooperate in neurite outgrowth promotion. J Cell Biol 135:1593–1607.

Buttiglione M, Revest JM, Rougon G, Faivre-Sarrailh C (1996) F3 neuronal adhesion molecule controls outgrowth and fasciculation of cerebellar granule cell neurites: a cell-type-specific effect mediated by the Ig-like domains. Mol Cell Neurosci 8:53–69.

Chai W, Yuen CT, Kogelberg H, Carruthers RA, Margolis RU, Feizi T, Lawson AM (1999) High prevalence of 2-mono- and 2,6-di-substituted manol-terminating sequences among O-glycans released from brain glycopeptides by reductive alkaline hydrolysis. Eur J Biochem 263:879–888.

Chen S, Mantei N, Dong L, Schachner M (1999) Prevention of neuronal cell death by neural adhesion molecules L1 and CHL1. J Neurobiol 38:428–439.

Chen YJ, Wing DR, Guile GR, Dwek RA, Harvey DJ, Zamze S (1998) Neutral N-glycans in adult rat brain tissue–complete characterisation reveals fucosylated hybrid and complex structures. Eur J Biochem 251:691–703.

Cheng W, Bullitt E, Bhattacharyya L, Brewer CF, Makowski L (1998) Electron microscopy and x-ray diffraction studies of *Lotus tetragonolobus A* isolectin cross-linked with a divalent Lewis^x oligosaccharide, an oncofetal antigen. J Biol Chem 273:35016–35022.

Crocker PR, Clark EA, Filbin M, Gordon S, Jones Y, Kehrl JH, Kelm S, Le Douarin N, Powell L, Roder J, Schnaar RL, Sgroi DC, Stamenkovic K, Schauer R, Schachner M, van den Berg TK, van der Merwe PA, Watt SM, Varki A (1998) Siglecs: a family of sialic-acid binding lectins. Glycobiology 8:v.

Curtis R, Green D, Lindsay RM, Wilkin GP (1993) Up-regulation of GAP-43 and growth of axons in rat spinal cord after compression injury. J Neurocytol 22:51–64.

Dityatev A, Brückner G, Dityateva G, Grosche J, Kleene R, Schachner M (2007) Activity-dependent formation and functions of chondroitin sulfate-rich extracellular matrix of perineuronal nets. Dev Neurobiol 67:570–588.

Faivre-Sarrailh C, Gauthier F, Denisenko-Nehrbass N, Le Bivic A, Rougon G, Girault JA (2000) The glycosylphosphatidyl inositol-anchored adhesion molecule F3/contactin is required for surface transport of paranodin/contactin-associated protein (caspr). J Cell Biol 149:491–502.

Falk J, Bonnon C, Girault JA, Faivre-Sarrailh C (2002) F3/contactin, a neuronal cell adhesion molecule implicated in axogenesis and myelination. Biol Cell 94:327–334.

Fukamauchi F, Aihara O, Wang YJ, Akasaka K, Takeda Y, Horie M, Kawano H, Sudo K, Asano M, Watanabe K, Iwakura Y (2001) TAG-1-deficient mice have marked elevation of adenosine A1 receptors in the hippocampus. Biochem Biophys Res Commun 281:220–226.

Gocht A, Struckhoff G, Lhler J (1996) CD15-containing glycoconjugates in the central nervous system. Histol Histopathol 11:1007–1028.

Haltiwanger RS, Lowe JB (2004) Role of glycosylation in development. Annu Rev Biochem 73:491–537.

Haspel J, Grumet M (2003) The L1CAM extracellular region: a multi-domain protein with modular and cooperative binding modes. Front Biosci 8:1210–1225.

Heller M, von der Ohe M, Kleene R, Mohajeri MH, Schachner M (2003) The immunoglobulin-superfamily molecule basigin is a binding protein for oligomannosidic carbohydrates: an anti-idiotypic approach. J Neurochem 84:557–565.

Jakovcevski I, Wu J, Karl N, Leshchyns'ka I, Sytnyk V, Chen J, Irintchev A, Schachner M (2007) Glial scar expression of CHL1, the close homolog of the adhesion molecule L1, limits recovery after spinal cord injury. J Neurosci 27:7222–7233.

Kadmon G, Eckert M, Sammar M, Schachner M, Altevogt P (1992) Nectadrin, the heat-stable antigen, is a cell adhesion molecule. J Cell Biol 118:1245–1258.

Karagogeos D (2003) Neural GPI-anchored cell adhesion molecules. Front Biosci 8:1304–1320.

Kleene R, Schachner M (2004) Glycans and neural cell interactions. Nat Rev Neurosci 5:195–208.

Kleene R, Yang H, Kutsche M, Schachner M (2001) The neural recognition molecule L1 is a sialic acid-binding lectin for CD24, which induces promotion and inhibition of neurite outgrowth. J Biol Chem 276:21656–21663.

Kleene R, Loers G, Langer J, Frobert Y, Buck F, Schachner M (2007) Prion protein regulates glutamate-dependent lactate transport of astrocytes. J Neurosci 27:12331–12340.

Kuhn TB, Stoeckli ET, Condrau MA, Rathjen FG, Sonderegger P (1991) Neurite outgrowth on immobilized axonin-1 is mediated by a heterophilic interaction with L1(G4). J Cell Biol 115:1113–1126.

Kunz S, Spirig M, Ginsburg C, Buchstaller A, Berger P, Lanz R, Rader C, Vogt L, Kunz B, Sonderegger P (1998) Neurite fasciculation mediated by complexes of axonin-1 and Ng cell adhesion molecule. J Cell Biol 143:1673–1690.

Mai JK, Krajewski S, Reifenberger G, Genderski B, Lensing-Höhn S, Ashwell KW (1999) Spatiotemporal expression gradients of the carbohydrate antigen (CD15) (Lewis X) during development of the human basal ganglia. Neuroscience 88:847–858.

Malhotra JD, Tsiotra P, Karagogeos D, Hortsch M (1998) *Cis*-activation of L1 mediated ankyrin recruitment by TAG-1 homophilic cell adhesion. J Biol Chem 273:33354–33359.

Maness PF, Schachner M (2007) Neural recognition molecules of the immunoglobulin superfamily: signaling transducers of axon guidance and neuronal migration. Nat Neurosci 10:19–26.

Nielsen PJ, Lorenz B, Müller AM, Wenger RH, Brombacher F, Simon M, von der Weid T, Langhorne WJ, Mossmann H, Köhler G (1997) Altered erythrocytes and a leaky block in B-cell development in CD24/HSA-deficient mice. Blood 89:1058–1067.

Niethammer P, Delling M, Sytnyk V, Dityatev A, Fukami K, Schachner M (2002) Cosignaling of NCAM via lipid rafts and the FGF receptor is required for neuritogenesis. J Cell Biol 157:521–532.

Olive S, Dubois C, Schachner M, Rougon G (1995) The F3 neuronal glycosylphosphatidylinositol-linked molecule is localized to glycolipid-enriched membrane subdomains and interacts with L1 and fyn kinase in cerebellum. J Neurochem 65:2307–2317.

Pavlou O, Theodorakis K, Falk J, Kutsche M, Schachner M, Faivre-Sarrailh C, Karagogeos D (2002) Analysis of interactions of the adhesion molecule TAG-1 and its domains with other immunoglobulin superfamily members. Mol Cell Neurosci 20:367–381.

Pearson WR (1990) Rapid and sensitive sequence comparison with FASTP and FASTA. Methods Enzymol 183:63–98.

Pillai AM, Garcia-Fresco GP, Sousa AD, Dupree JL, Philpot BD, Bhat MA (2007) No effect of genetic deletion of contactin-associated protein (CASPR) on axonal orientation and synaptic plasticity. J Neurosci Res 85:2318–2331.

Poliak S, Salomon D, Elhanany H, Sabanay H, Kiernan B, Pevny L, Stewart CL, Xu X, Chiu SY, Shrager P, Furley AJ, Peles E (2003) Juxtaparanodal clustering of Shaker-like K+ channels in myelinated axons depends on Caspr2 and TAG-1. J Cell Biol 162:1149–1160.

Rader C, Kunz B, Lierheimer R, Giger RJ, Berger P, Tittmann P, Gross H, Sonderegger P (1996) Implications for the domain arrangement of axonin-1 derived from the mapping of its NgCAM binding site. EMBO J 15:2056–2068.

Rios JC, Melendez-Vasquez CV, Einheber S, Lustig M, Grumet M, Hemperly J, Peles E, Salzer JL (2000) Contactin-associated protein (Caspr) and contactin form a complex that is targeted to the paranodal junctions during myelination. J Neurosci 20:8354–8364.

Sajdel-Sulkowska EM (1998) Immunofluorescent detection of CD15-fucosylated glycoconjugates in primary cerebellar cultures and their function in glial-neuronal adhesion in the central nervous system. Acta Biochim Pol 45:781–790.

Salzer JL (2003) Polarized domains of myelinated axons. Neuron 40:297–318.

Shewan D, Calaora V, Nielsen P, Cohen J, Rougon G, Moreau H (1996) mCD24, a glycoprotein transiently expressed by neurons, is an inhibitor or neurite outgrowth. J Neurosci 16:2624–2634.

Simova O, Irintchev A, Mehanna A, Liu J, Dihné M, Bächle D, Sewald N, Loers G, Schachner M (2006) Carbohydrate mimics promote functional recovery after peripheral nerve repair. Ann Neurol 60:430–437.

Sonderegger P (1997) Axonin-1 and NgCAM as "recognition" components of the pathway sensor apparatus of growth cones: a synopsis. Cell Tissue Res 290:429–439.

Streit A, Yuen CT, Loveless RW, Lawson AM, Finne J, Schmitz B, Feizi T, Stern CD (1996) The Le. (x) carbohydrate sequence is recognized by antibody to L5, a functional antigen in early neural development. J Neurochem 66:834–844.

Traka M, Goutebroze L, Denisenko N, Bessa M, Nifli A, Havaki S, Iwakura Y, Fukamauchi F, Watanabe K, Soliven B, Girault JA, Karagogeos D (2003) Association of TAG-1 with Caspr2 is essential for the molecular organization of juxtaparanodal regions of myelinated fibers. J Cell Biol 162:1161–1172.

Tzimourakas A, Giasemi S, Mouratidou M, Karagogeos D (2007) Structure-function analysis of protein complexes involved in the molecular architecture of juxtaparanodal regions of myelinated fibers. Biotechnol J 2:577–583.

Vinson M, van der Merwe PA, Kelm S, May A, Jones EY, Crocker PR (1996) Characterization of the sialic acid-binding site in sialoadhesin by site-directed mutagenesis. J Biol Chem 271:9267–9272.

Vinson M, Strijbos PJ, Rowles A, Facci L, Moore SE, Simmons DL, Walsh FS (2001) Myelin-associated glycoprotein interacts with ganglioside GT1b. A mechanism for neurite outgrowth inhibition. J Biol Chem 276:20280–20285.

Wenger RH, Kopf M, Nitschke L, Lamers MC, Köhler G, Nielsen PJ (1995) B-cell maturation in chimaeric mice deficient for the heat stable antigen (HSA/mouse CD24). Transgenic Res 4:173–183.

Yamamoto K, Konami Y, Osawa T, Irimura T (1992) Carbohydrate-binding peptides from several anti-H(O) lectins. J Biochem 111:436–439.